Wildfires in polluted areas: mineralogical transformations and remobilization of metal(loid)s

Marek Tuhý

Supervised by prof. RNDr. Vojtěch Ettler, Ph.D.

Institute of Geochemistry, Mineralogy and Mineral Resources
Faculty of Science
Charles University

A dissertation submitted for the degree of
Doctor of Philosophy

Prague, 2021

Declaration of the author/Prohlášení autora:

I declare that this Ph.D. thesis was written by myself and that all the literary sources were cited properly. Neither this work, nor the substantial part of it was used to reach the same or any other academic degree.

Prohlašuji, že jsem předkládanou disertační práci vypracoval samostatně a že všechny použité literární zdroje jsou řádně uvedeny. Dále prohlašuji, že tato práce ani její podstatná část nebyla předložena k získání stejného či jiného akademického titulu.

In Prague, July 2021

V Praze, červenec 2021

…….

Marek Tuhý

Acknowledgments

Foremost, my sincerest thanks go to my supervisor, Professor Vojtěch Ettler. Not only did he provide me an excellent opportunity to investigate such an exciting topic and led my Ph.D. project, but he has encouraged and inspired my future work in science. I appreciate the endless and fruitful discussions, his trust and kind support. I could not have imagined having a better advisor and mentor for my Ph.D. study.

My special thanks go to Dr. Jan Rohovec for his innovative ideas, enthusiasm for my research, and highly beneficial help. Collaborating with him and Dr. Šárka Matoušková gave me valuable experience in the laboratory and taught me the importance of interdisciplinary cooperation.

I am also very grateful to Professor Juraj Majzlan, who facilitated measurements at the synchrotron in Karlsruhe and aided the ongoing project. The mentorship of Professor Martin Mihaljevič has inspired me since my early studies. Also, acknowledgments to my collaborators and colleagues, Dr. Martin Racek for the EPMA analyses, Associate Professor Petr Drahota for the XRD measurements and Marie Fayadová for the laboratory help. Additionally, to all the people at my home institute, thank you for setting a friendly and professional ambiance.

I would like to express my special thanks to my family (namely my mother Jitka, father Radek, brother Vítek, and grandparents Hanka, Zdeňka, and Pepa) for their unconditional support, interest and patience during my studies.

Mr. Alan Harvey Cook is thanked for his review of the English in this Ph.D. thesis.

This study was supported by the Czech Science Foundation (GAČR project no. 19-18513S) and a student grant attributed to Marek Tuhý from the Grant Agency of Charles University (GAUK 1598218), and partially funded by the Center for Geosphere Dynamics (UNCE/SCI/006).

Summary

Wildfires contribute to the global emissions of trace elements. This Ph.D. thesis focuses on highly polluted areas near smelting/mining polluted sites in Africa, where wildfires are frequent. Experimental samples corresponding to both representative biomass-rich topsoils and grass were investigated using a combination of mineralogical and geochemical methods. Wildfires were simulated using a thermodesorption (TD) technique (75-670 °C; Hg) and newly introduced experimental set-ups (250-850 °C), enabling the online detection of the released contaminants and the sampling the aerosols and ashes. The subsequent investigation revealed the mineralogical and chemical transformations necessary for understanding the temperature-dependent releases of the metal(loid) contaminants during the simulated wildfire.

The thermodesorption experiments indicated that >90 % of Hg was released at ~340 °C. A comparison with the Hg reference compounds' TD curves confirmed that the Hg in the biomass-rich topsoils occurs as a mixture of the Hg bound to the organic matter and nanocrystalline black HgS, which exhibited similarities with the TD pattern of smelter flue dust residue. The release of the other metal(loid)s from the topsoils (As, Cd, Cu, Pb, Zn) is dependent on their solid-state speciation, which was determined by the autoSEM method. Metals (Cd, Cu, Pb, Zn) were released at temperatures >550 °C and were mainly retained in the ash. In contrast, As exhibited several emission peaks at ~275 °C, ~370–410 °C, and ~580 °C, reflecting its complex speciation in the solid phase. Wildfire simulating experiments enabled one to quantify the potential 'worst-case scenario' releases of the metal(loid)s. At 850 °C, up to 5–14 % As, 2–12 % Cu, 3–17 % Pb, 2–20 % Zn and 27–79 % Cd of the total was released from the most contaminated topsoils. It is, therefore, evident that such polluted sites deserve attention and protection against wildfires to limit the potential emissions of trace metal(loid) contaminants. This thesis clearly shows that the adopted experimental set-ups, when combined with detailed geochemical/mineralogical investigations, represent useful tools for deciphering the fate of contaminants in wildfire-affected areas and should be combined with field investigations in the future.

Abstrakt

Požáry se podílejí na globálních emisích stopových prvků. Tato doktorská práce se zabývá oblastmi Afriky, které jsou silně znečištěné těžbou a hutnictvím kovů, a navíc jsou často vystavené požárům. Experimentální vzorky svrchních půd bohatých na biomasu i travních porostů byly charakterizovány pomocí mineralogických/geochemických metod. Následně byly prováděny experimenty simulující požáry, a to pomocí termodesorpčních technik (75-670 °C; v případě Hg) a nově navržených experimentálních aparatur (250-850 °C), které umožňují online detekci uvolňovaných kontaminantů a vzorkování uvolňovaných aerosolů i popela. Současně byly zkoumány mineralogické/chemické transformace, které jsou stěžejní pro správné pochopení uvolňování kontaminantů během simulovaných požárů.

Z termodesorpčních experimentů vyplývá, že více než 90 % Hg je remobilizováno již při teplotách okolo 340 °C. Porovnáním získaných termodesorpčních křivek vzorků s křivkami referenčních materiálů bylo zjištěno, že Hg se ve svrchních půdách vyskytuje zejména vázaná na organickou hmotu, případně ve formě nanokrystalického metacinabaritu (HgS), který byl detekován i ve vzorcích popílku z huti. Uvolňování ostatních (polo)kovů (As, Cd, Cu, Pb, Zn) je silně závislé na jejich speciaci v pevné fázi, která byla zkoumána pomocí automatické mineralogie. Kovy (Cd, Cu, Pb, Zn) byly převážně koncentrovány v popelu a k jejich částečnému uvolňování docházelo až za teplot přesahujících 550 °C. Oproti tomu As byl uvolňován v několika teplotních intervalech: ~275 °C, ~370–410 °C a ~580 °C, což souvisí s velmi pestrou minerální/fázovou asociací ve studovaných materiálech. Pomocí těchto experimentů bylo možné kvantifikovat emise kontaminantů během nejintenzivnějších požárů. Při požáru dosahujícího teploty 850 °C by se z celkového množství v znečištěných svrchních půdách uvolnilo 5–14 % As, 2–12 % Cu, 3–17 % Pb, 2–20 % Zn a 27–79 % Cd. Z těchto zjištění je zřejmé, že těžbou znečištěné oblasti je třeba chránit před požáry zejména proto, aby se zabránilo emisím kontaminantů. Z výsledků této práce je patrné, že tyto experimentální přístupy jsou vhodné ke studiu chování (polo)kovů během požárů v kontaminovaných oblastech, zvláště v kombinaci s ostatními geochemickými/mineralogickými metodami. Další výzkumy zabývajícími se těmito procesy by v budoucnosti měly být doplněny také experimentálními požáry přímo v terénu.

Contents

List of Annexes

I **Tuhý, M.**, Hrstka, T., Ettler, V., 2020. Automated mineralogy for quantification and partitioning of metal(loid)s in particulates from mining/smelting-polluted soils. *Environmental Pollution* 266: 115118. https://doi.org/10.1016/j.envpol.2020115118

II **Tuhý, M.**, Rohovec, J., Matoušková, Š., Mihaljevič, M., Kříbek, B., Vaněk, A., Mapani, B., Göttlicher, J., Steininger, R., Majzlan, J., Ettler, V., 2020. The potential wildfire effects on mercury remobilization from topsoils and biomass in a smelter-polluted semi-arid area. *Chemosphere* 247: 125972. https://doi.org/10.1016/j.chemosphere.2020.125972

III **Tuhý, M.**, Ettler, V., Rohovec, J., Matoušková, Š., Mihaljevič, M., Kříbek, B., Mapani, B., 2021. Metal(loid)s remobilization and mineralogical transformations in smelter-polluted savanna soils under simulated wildfire conditions. *Journal of Environmental Management* 293: 112899. https://doi.org/10.1016/j.jenvman.2021.112899

IV **Tuhý, M.**, Ettler, V., Rohovec, J., Matoušková, Š., Mihaljevič, M., Kříbek, B., Mapani, B., 2021. Wildfires remobilize metal(loid)s from contaminated grass in mining areas of sub-Saharan Africa. (unpublished data)

V **Tuhý, M.**, Ettler, V., 2020. Přírodní požáry a remobilizace kovů. *Vesmír* 99: 458-460.

1 Introduction

Wildfires have been an integral part of the terrestrial ecosystem for more than 400 million years. As reported through sedimentary rocks, the wildfire frequency was directly proportional to the rising oxygen content in the atmosphere (Scott et al., 2018). Humankind benefited from fires for thousands of years. Approximately 300,000 years ago, man started to intentionally use fire on a daily basis as a tool for self-defense, as a source of light, and subsequently also as a weapon. Humans also used fire to transform forests into animal-rich open grasslands, where hunting was easier (Harari, 2015).

In specific environments, wildfires might help to maintain the overall ecosystem sustainability. As an example, the Australian eucalyptus (genus: *Eucalyptus*) is directly dependent on wildfire activity, it releases terpenoids from its leaves, possibly to promote ignition (Jones and Raj, 1988). Additionally, the released heat helps the seeds to germinate and reduces the competing plants. Moreover, the eucalyptus developed the ability to efficiently resprout even after fire events (Crisp et al., 2011). A similar situation might be found in African savannas, which need fires to thrive. The savanna's existence and its biodiversity are partially ensured

by an occasional wildfire (Beale et al., 2018, Stavel et al., 2011). Again, fire promotes seed germination, kills pests, and returns nutrients back into the soil (Hassan et al., 2008; Butz, 2009; Pausas and Keeley, 2019). As a result, controlled burning, fuel reduction burns, and prescribed fires are used in many places around the world. Despite all these benefits, wildfires might cause the emission of greenhouse gases, increase soil erosion, or negatively influence soil biota. Moreover, wildfires do not avoid contaminated places and might cause the remobilization of inorganic contaminants (metals and metalloids) (Gaudichet et al., 1995; Isey and Taylor, 2020; Kayee et al., 2020; Jahn et al., 2021). Given the fact that the latter phenomenon has not been extensively studied thus far, this Ph.D. thesis focuses on the effects of fires on contaminated biomass-rich soil systems.

2 Wildfires in the environmental systems

2.1 Wildfire frequency and occurrence

Since the wildfire frequency is rising, understanding the wildfires' effects on the environment is becoming of great importance nowadays. One of the possible explanations might be the influence of climate change, which increases the vulnerability of ecosystems to fire (Pereira et al., 2019; Sankey et al., 2017). **Figure 1** shows the increasing fire frequency on an example from the western USA in both forested and grassland areas (Westerling, 2016). Evidence of this phenomenon might be found in the interest of a broad scientific community resulting in both many publications and special issues of magazines such as *Philosophical Transactions B* (Scott et al., 2016), *Science of the Total Environment* (Úbeda et al., 2018), *Journal of Environmental Monitoring* (Muñoz-Rojas and Pereira, 2019), and books (Pereira et al., 2019).

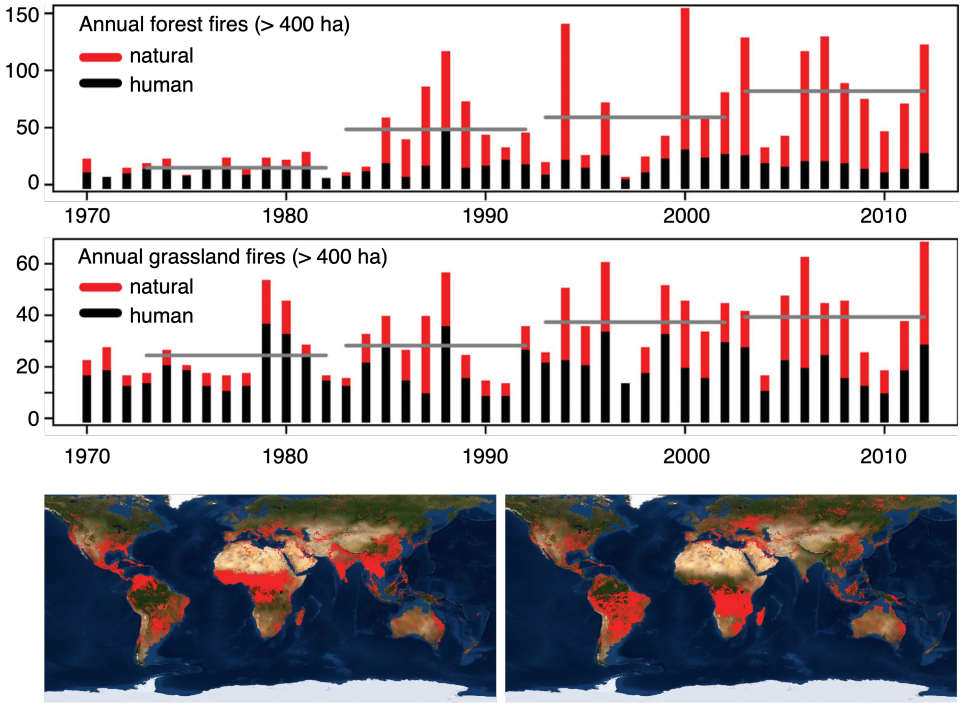

Figure 1. Compilation of graphs illustrating the annual increase of forest and grassland fires, both natural and human-caused, documented by the Forest Service, Park Service and Indian Lands in the western USA (adapted from Westerling, 2016) and coupled with the NASA FIRMS satellite images showing detected fire events in February 2020 (bottom left) and in August 2020 (bottom right) (accessed on May 11, 2021).

The terminology related to natural fires (wildfires) and their environmental effects are often contradictory or unclear. For this reason, **Box 1** shows the fundamental terminology on this topic compiled from the literature.

Box 1. Basic terminology (natural fires and fire effects)

A wildfire is an uncontrolled or naturally occurring fire (Shakesby and Doer, 2006) and is associated with several important keywords. According to Smith et al. (2005), the **fire intensity,** as one of the key fire-descriptions, might be explained as the rate of heat produced per unit area affected by a fire. The fire intensity could be quantified as the rate of spread (burned meters per second) coupled with the energy flux (generated kilowatts per burned meter) and is typically reported in kJ/m^2 (Lentile et al., 2006).

Fire severity definitions vary, but might be interpreted as 'the magnitude of ecological change of the fire' (Lentile et al., 2006). It simply describes how the fire intensity affects the ecosystems (Keeley et al., 2009; Pereira et al. 2019).
The classification of the fire effects, per Ryan and Noste (1985), is the following:

- *Unburned*
- *Scorched* (unburned, but radiated)
- *Light* (trees still have green leaves, no deep soil affection)
- *Moderate or severe surface burn* (trees exhibit canopy damage, largely consumed soil organic layer)
- *Deep burning or crown fire* (canopy trees consumed, soil organic layer consumed, white ash deposition, charred organics to a depth of centimeters)

In contrast, the **burn severity** relates to the amount of time necessary to return to pre-fire levels or functions (Lentile et al., 2006).

Lentile et al. (2006) noted that a grassland fire consumes large portions of the biomass, which would represent a high fire severity. However, on the other hand, grasslands rejuvenate quite quickly, which indicates an overall low fire severity.

2.2 Experimental investigations of wildfires

Wildfires influence the soils' physical properties (e.g., Shakesby and Doerr, 2006; Araya et al., 2016). As post-fire land is more prone to erosion (Sankey et al., 2017), in combination with rainfall, post-fire

debris flows might cause damage to the infrastructure and can result in the loss of human lives (Jordan, 2016; Shakesby and Doerr, 2016; Pereira et al., 2019). According to Campos et al. (2016), wildfires cause the enrichment in both the major and trace elements in the residual ash, resulting in a risk of the subsequent remobilization of contaminants by water (in agreement with Abraham et al., 2017). All these mentioned risks are the major reasons for the experimental investigations of wildfires and their environmental effects.

Wildfire impacts might be studied both directly in the field or using laboratory simulations. Direct wildland fire studies are limited to experimental fires that allow the preinstallation of measuring equipment (Miranda et al., 1993; Stephens et al., 2005; Úbeda et al., 2018; **Figure 2a, b**) or must be determined indirectly via observing the wildfire consequences (Pereira et al., 2019). Soil heating measurements are usually performed using thermosensitive paints (recording the maximum temperature reached; Cawson et al., 2016) or thermocouples connected to data loggers (providing temperature-time dependency; Miranda et al., 1993). Wildfire temperatures and the corresponding ash colors are shown in **Box 2**. Conventionally, wildfire laboratory simulations have been performed in simple muffle furnaces (**Figure 2c**; e.g., Johnston et al., 2019,

Araya et al., 2016; Úbeda et al., 2009). Some of the fire studies have also been performed using blowtorches (Badía-Villas et al. 2014, Aznar et al., 2016) and infrared heating (Cancelo-Gonzáles et al., 2014), where the main advantage was the application of the heat directly to the surface of the soil column (Pereira et al., 2019). The Pyrotron experimental device represents an innovative set-up based in Australia (CSIRO Pyrotron facility, **Figure 2d**) and allows laboratory-based large-scale wildfire experiments. It consists of a 25-m long metal tunnel equipped with a fan, LPG/ethanol ignition sources, viewing doors/windows, several sensors (such as thermocouples) and high-speed and infra-red thermal imaging cameras and emissions samplers (https://www.csiro.au/en/work-with-us/use-our-labs-facilities/pyrotron-facility; Gould, 2017; Sullivan, 2017; Howard et al., 2019).

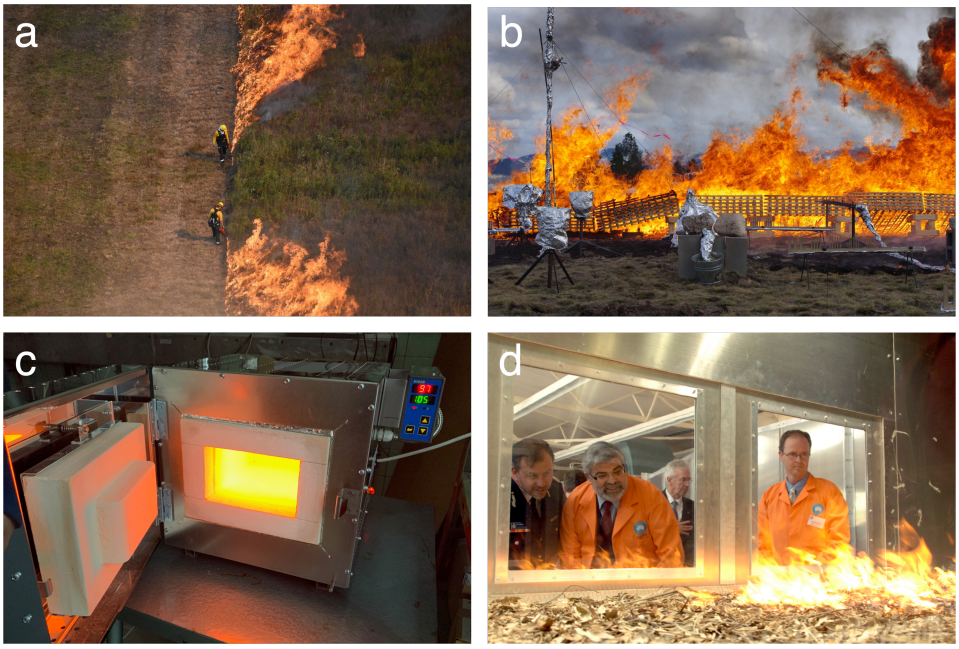

Figure 2. a) Prescribed burning performed by the Wisconsin Department of Natural Resources (DNR) in order to control invasive species (https://dnr.wisconsin.gov/newsroom/release/40611); b) Controlled fire experiment (https://www.usgs.gov/media/images/controlled-fire-studies-provide-data-archaeological-sites-impacts); c) Muffle furnace conventionally used for burning experiments (photo: M. Tuhý); d) Ongoing experiment in the Pyrotron laboratory (https://www.scienceimage.csiro.au/).

Box 2. Wildfire temperatures, time and ash colors

Wildfire temperatures and the time of exposure correspond to fuel properties and climate conditions. Generally, temperatures vary in the range of 50–1500 °C (Neary et al., 1999). A huge contrast in the temperatures and the time of combustion might be observed between grassland fires and forest fires. In general, grassland fire temperatures reach approximately 300–350 °C for a short period of time (roughly minutes), but temperatures during a forest litter fire reach 500 °C and last for hours.

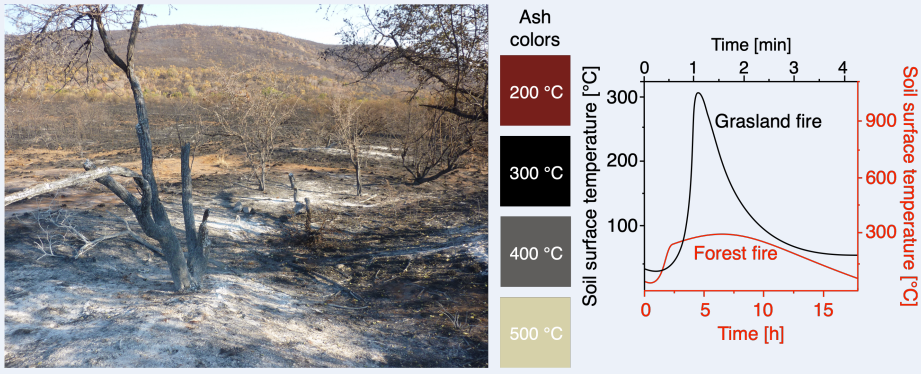

A burned area in Pilanesberg National Park (South Africa; photo: V. Ettler) with a typical patchy ash color distribution showing the different burning temperatures dependent on the fuel type. The ash color chart was taken from Bento-Gonçaves et al. (2012) and shows the ash color and temperature dependence as obtained by burning cork oak (*Quercus suber*) leaf litter from Albufeira (Portugal). The graph was adapted from Ryan et al. (2002) and indicates that grassland fires reach temperatures around 300 °C just for minutes compared to forest fires where the uppermost soil layer is heated to nearly the same temperatures, but in the time scale of hours.

2.3 Wildfires in contaminated sites

The processes resulting in contaminants emissions during wildfires have been poorly studied, although in 1989, Nriagu estimated the wildfire contribution to the overall metal(loid)s emissions to be 1900 t Pb, 7600 t Zn, 3800 t Cu, 190 t As and 110 t Cd per year. Several studies have

been performed to decipher the wildfire-driven emissions of Hg and showed Hg volatility even under moderate fire conditions (Wiedinmeyer and Friedli, 2007; Navrátil et al., 2009; Campos et al., 2015, Abraham et al., 2018a). Other trace elements, including Cu, Zn, Pb, and Cd, were detected in biomass burning-derived aerosols as demonstrated by studies from the African savanna (Gaudichet et al., 1995), Australia (Isley and Taylor, 2020), the USA (Jahn et al., 2021) and Asia (Kayee et al., 2020), where wildfires are quite frequent.

The mentioned works dealt with wildfires in typical fire-exposed areas. However, investigations of wildfire effects in sites polluted by anthropogenic activities, combined with advanced mineralogical and phase transformations studies and overall mass-balance calculations, seem to be almost non-existent in the scientific literature. However, as demonstrated in the examples in **Figures 3a** and **3b**, wildfires might even occur next to mining/smelting centers.

Figure 3. Wildfires in semi-arid African savannas. a) Spot wildfire visible from a plane in the vicinity of a gold mine near Johannesburg (Republic of South Africa), b) Grassland wildfire in the Tsumeb mining area (Namibia), c) Lightning-initiated wildfire near Monate Private Game Reserve (Limpopo district, Republic of South Africa), d-e) Post-wildfire bush in Pilanesberg National Park (Republic of South Africa), f) Grassland after a human-initiated fire near an inhabited area (Gauteng district, Republic of South Africa). [Authors of photos: V. Ettler (a, b, d), E. Schronda (c), M. Tuhý (e, f)].

Furthermore, isotopic investigations of the ash from wildfires in the USA and Australia have shown that the industrial Pb from gasoline combustion was clearly present (Odigie and Flegal, 2011, 2014; Kristensen and Taylor, 2014; Wu et al., 2017). Other studies from Australia compared the Pb isotopic compositions of aerosols before, during, and after wildfire periods; the authors found that the interpretation of the Pb isotopic patterns is not straightforward, but the contribution of remobilized anthropogenic Pb seems to occur (Kristensen et al., 2017; Isley and Taylor, 2020).

At many places in the vicinity of active and abandoned mines and non-ferrous metal smelters, soils exhibit extremely high concentrations of metals and metalloids, commonly in the range of thousands to tens of thousands mg/kg (see Ettler, 2016 for a compilation). The examples include Kitwe (Zambia, Ettler et al., 2011), Mufulira (Zambia, Ettler et al., 2016), Newcastle (Australia, Harvey et al., 2017) or Příbram (Czech Republic, Rieuwerts et al., 1999).

Abraham et al. (2018a, b) stressed the risk of wildfire-driven contaminant remobilization into the environment in contaminated semi-arid mining/smelting areas. A large variety of both anthropogenic and geogenic particles are released into the environment because of the ore mining

and smelting. These particles, often containing contaminant-bearing phases, might be considered as pollutants of soil systems, surface water and the air (Beavington et al., 2004). In the mining and smelting areas, the wind represents the main transporter of metal(loid)-bearing particles, which can travel a large distance, often more than 100 km (Hou et al., 2006). **Figure 4** shows where wildfires occurred in January 2020 in a contaminated area near the Mount Isa smelter (Australia).

The particles transported by the wind may also adhere to the surfaces of vegetation. Afterward, they are deposited onto the soil surface as leaf litter and are incorporated into the topsoil organic matter (**Figure 5a, b**; Kříbek et al., 2016). Particulates emitted by mining and smelting industries or windblown from waste disposal sites have very complex chemical and mineralogical compositions (**Figure 5c, d**; Ettler et al., 2016). Several studies from Cu mining areas in Zambia showed lower concentrations of contaminants in the wooded plots compared to the grasslands, despite the expected higher retention of particulates by the trees' canopies (Mihaljevič et al., 2011; Ettler et al., 2014). The authors hypothesized that more intense fires beneath the trees might be responsible for this phenomenon due to the greater re-emission of metals as compared to that in the grasslands.

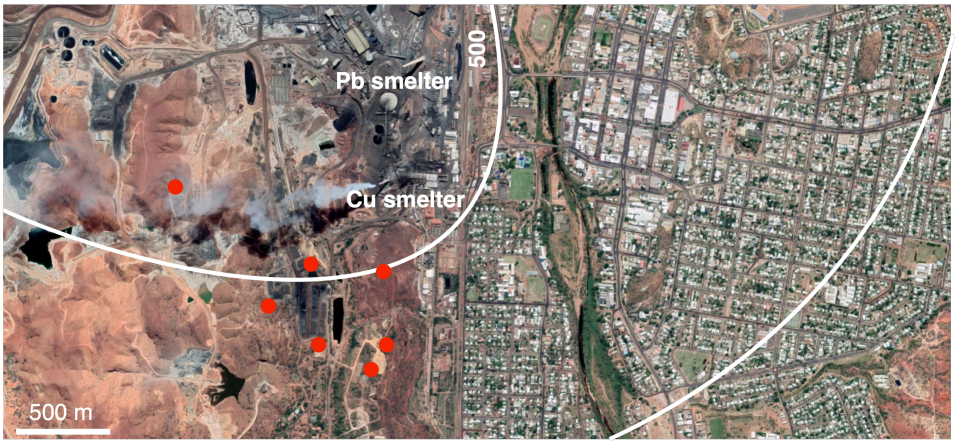

Figure 4. The surroundings of a metallurgical site in Mount Isa (Australia), showing the chimney smoke from the Cu smelter. The isolines define the annual deposition rate of lead (500 and 200 mg/m^2/year) according to Wilson (2018). The red dots represent the individual detected spot fires during the extensive fire period in January 2020 (Fire Watch Landgate, https://firewatch-pro.landgate.wa.gov.au). The map was acquired from Google Maps (23. 1. 2020) (modified from **Annex V**).

Africa is a continent bearing many mineral resources ranging from diamonds to metals, which are critical for today's industries (U.S. Geological Survey, Mineral Commodity Summaries, 2020). Moreover, according to fire-monitoring systems (NASA FIRMS, **Figure 1**), wildfires are quite frequent during dry periods of the year when African ecosystems are more vulnerable to fire. Therefore, environments near mines and smelters in Africa represent convenient geochemical laboratories for studying the wildfire impact with a special emphasis on the potential contaminant remobilization.

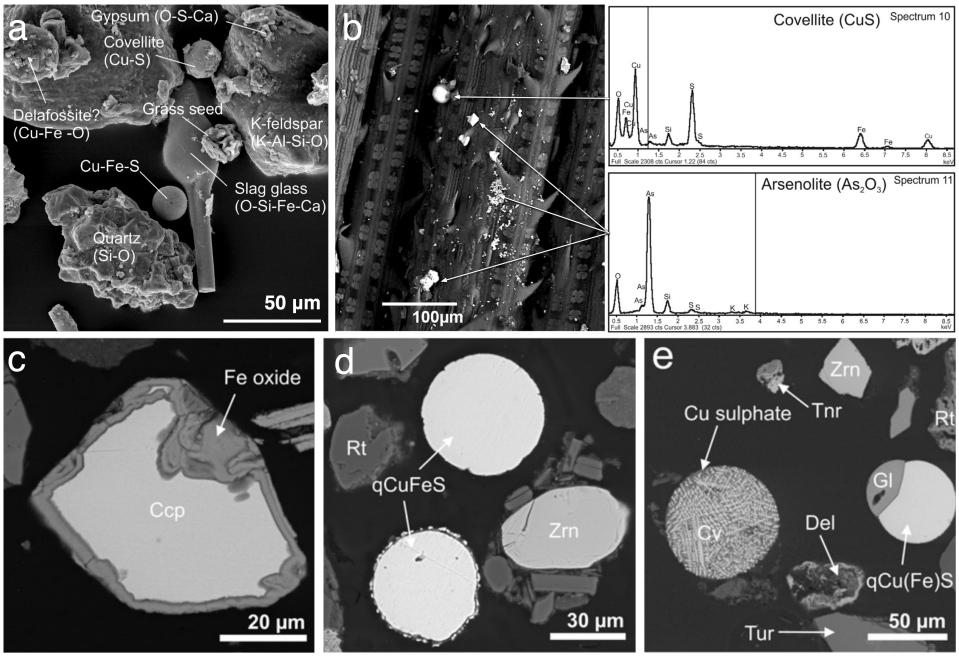

Figure 5. Scanning electron micrographs of mining- and smelter-derived particles adhering to biomass surfaces (a-b; Tsumeb, Namibia, adapted from Kříbek et al., 2016) and found in the soil heavy mineral fractions (c-e; Mufulira, Zambia, adapted from Ettler et al., 2016). a) Dust particles collected from grass showing the association of geogenic minerals [quartz (SiO_2), K-feldspar ($KAlSi_3O_8$), gypsum ($CaSO_4 \cdot H_2O$)] with anthropogenic particles [spherical particles of slag glass (various composition), spherical covellite (CuS)]; b) Covellite and arsenolite (As_2O_3) dust particles directly adhering to the grass twigs with appropriate EDS spectra; c) Mine tailing-derived chalcopyrite (Ccp, $CuFeS_2$) with an alteration rim composed of Fe oxides; d) Smelter-derived spherical particles in association with geogenic zircon (Zrn, $ZrSiO_4$) and rutile (Rt, TiO_2); e) Spherical covellite (Cv) particle with Cu-sulfate and spherical quenched Cu(Fe)S phase associated with zircon, rutile, tenorite (Tnr, CuO), delafosite (Del, $CuFeO_2$) and tourmaline [Tur, mainly schorl: $NaFe_3Al_6Si_6O_{18}(BO_3)_3(OH)_4$)].

Therefore, we decided to investigate the potential wildfire effects on contaminants in highly polluted environmental samples (soils, biomass) near several active and abandoned mining and smelting sites in sub-Saharan Africa. We hypothesized that wildfires remobilize part

of the contaminants from the topsoils and the degree of remobilization is mainly controlled by the temperature and speciation of the metal(loid)s. Therefore, the research questions were the following:

(i) Are the selected contaminants (e.g., As, Cd, Cu, Pb, Zn) during wildfires remobilized into the atmosphere?

(ii) If so, what is the percentage of total contaminant released?

(iii) Considering the known Hg sensitivity to be volatilized, can the Hg be fully remobilized during potential wildfires in the studied areas?

(iv) Is the sensitivity of the metal(loid)s to be volatilized also controlled by their speciation in the solid phase?

(v) Are there any changes in the contaminants' speciation during combustion?

(vi) Finally, considering these experimental results, can we potentially assess the overall risk of wildfires in smelting/mining contaminated sites?

The aims of the thesis were to:

1. Adopt and optimize the automated mineralogy technique (autoSEM) for highly complex mining- and smelter-polluted topsoils to decipher the metal(loid) partitioning within the individual phases, necessary for further interpretations of wildfire simulations.
2. Design and test the experimental wildfire simulation set-up with continuous air delivery enabling one to sample the aerosol, ashes and outcoming gases.
3. Conduct burning experiments on the soil and biomass samples in the temperature ranges relevant for wildfires in semi-arid areas to estimate the remobilization potential of the key metal(loid)s (As, Cd, Cu, Hg, Pb, Zn).

3 Experimental approach

3.1 Sample description

For this investigation, experimental topsoil samples mainly from the Tsumeb mining/smelting area in northern Namibia (19°15'S, 17°42'E) were used. The history of the ore mining and processing dates back more than 100 years there. Currently, the mines are closed, the Pb smelter is being dismantled, but the former Cu smelter was upgraded to be able to process complex Cu concentrates (including As-rich ones), as one of a few in the world. The Tsumeb smelter currently employs approximately 800 people and is owned by the Canadian company Dundee Precious Metals. In 2020, the smelter processed 232,000 tons of Cu concentrate mainly from Chelopech (Bulgaria), El Brocal (Peru), Codelco (Chile), Armenia and Opuwo (Namibia) (Dundee Precious Metals, https://www.dundeeprecious.com).

In July 2013, the experimental biomass-rich topsoils from Tsumeb were sampled in a polluted hotspot adjacent to the smelter and waste disposal sites on the lee side of the prevailing winds. The experimental topsoils were developed under the most common vegetation cover in the area: A – *Acacia* spp., AM – *Acacia* spp. and the marula tree (*Sclerocarya birrea*) and G –

grass (*Aristida stipitata*). The samples were air-dried and transported to the laboratory, sieved into fractions <2 mm, 2-5 mm and >5 mm and disaggregated in a cutting machine (Fritsch Pulverisette 14). It has already been demonstrated that metal(loid)-bearing phases are dominantly found in the heavy mineral fractions (e.g., Ettler et al., 2016). The fraction <2 mm, which was the most enriched in the metal(loid)s and metal(loid)-bearing particles, was used for further experimental work.

Biomass samples from several other abandoned smelting areas in sub-Saharan Africa were used to decipher the potential remobilization of the metal(loid)s by the biomass burning during wildfires in grasslands. The grass samples were collected in Selebi-Phikwe in Botswana (Ni-Cu mine and smelter; 21°56'43.2"S 27°50'36.0"E), Luanshya in the Zambian Copperbelt (Cu mine and smelter; 13°07'60.0"S 28°23'20.0"E), and Kabwe in central Zambia (Pb-Zn mine and smelter; 14°27'33.4"S 28°25'36.4"E). Additional grass samples (n = 30) and topsoils (n = 28) were collected in the larger Tsumeb area to determine the spatial distribution of the Hg and its potential fluxes during the wildfire-driven remobilization (**Annex II** and corresponding Supplementary Material). The positions of all the sampling sites are plotted in **Figure 6** and photographs of the individual localities are given in **Annex IV**.

The Ni-Cu deposit Selebi Phikwe is located in eastern Botswana. The Köppen Climate Classification subtype is "Bsh" (Mid-Latitude Steppe and Desert Climate; average temperature of 21 °C, average precipitation of around 450 mm) (Šráček et al., 2018). The key metal-hosting minerals are pyrrhotite ($Fe_{1-x}S$), pyrite (FeS_2), pentlandite [$(Fe,Ni)_9S_8$] and chalcopyrite ($CuFeS_2$) (Maier et al., 2008). The mines and a Cu-Ni smelter equipped with the flash furnace smelting technology were in operation from 1973 to 2016.

The Kabwe smelting/mining area in central Zambia is considered as one of the most polluted cities in the world. The local mine, operated from 1906 to 1994, produced 0.8 Mt Pb, 1.8 Mt Zn and to a lesser extent Ag, V, Cd and Cu (Kamona and Friedrich, 2007). The smelters were in operation until the mine closure in 1994, but left large dumps with more than 2.5 Mt of granulated slag deposited in the former mine area. The key metal-hosting minerals are galena (PbS), pyrite (FeS_2), sphalerite (ZnS), and chalcopyrite ($CuFeS_2$). The Köppen Climate Classification corresponds to "Cfa" (Humid Subtropical Climate). According to Tembo et al. (2006), the local soils have been classified as highly polluted.

The Cu mine in Luanshya was the first large-scale Cu mine in the Zambian Copperbelt that has been operating since 1928 (Sikamo et al., 2016). The current owner, China Nonferrous Metal Mining Corporation (CNMC) still operates an open pit mine in the area. The ore is dominantly composed of pyrite (FeS_2), chalcopyrite ($CuFeS_2$), bornite (Cu_5FeS_4), linnaeite (Co_3S_4), and carrollite [$Cu(Co,Ni)_2S_4$] (Kamona and Nyambe, 2002). The smelter was established in 1932, operating several reverbatory furnaces and Peirce-Smith converters, and was shut down in 1999. The local environment is highly polluted by Cu (>2200 mg/kg) and Cd (>60 mg/kg) (Kříbek et al., 2010).

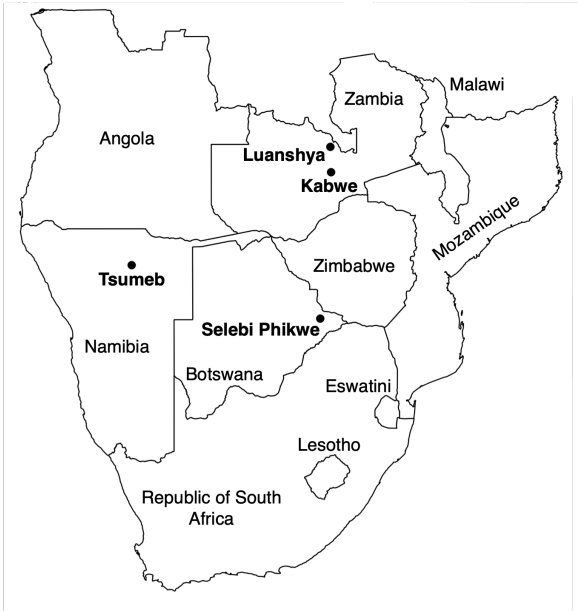

Figure 6. Map of south Africa with the indicated of the study sites.

3.2 Determination of bulk chemistry

A detailed mineralogical and geochemical investigation of soil and biomass samples is required to obtain information about the sample composition and metal(loid) speciation. This information is necessary to adequately interpret the results obtained by the wildfire-simulating experiments. Primarily, the knowledge of the total concentrations of the selected elements, including the metal(loid)s, is needed. Apart from microwave-assisted digestions, conventional digestion methods used for soils and organic-rich materials are generally performed in open systems. This approach consists of an ashing step in a muffle furnace, applied to reduce the amount of organic matter in a sample and to facilitate the further dissolution in the mineral acids. However, for the interpretation of wildfire-simulation experiments, the exact knowledge of the metal(loid) concentrations in the unburned samples is of key importance. Therefore, combustion-free digestion in a closed system was suggested and tested (**Box 3**). The digests obtained by this method were analyzed by a combination of inductively coupled plasma (ICP) optical emission spectrometry (OES) and mass spectrometry (MS) (**Box 4**). The total Hg content was determined using conventional cold vapor atomic absorption spectroscopy CV-AAS (AMA 254).

Box 3. Bulk chemistry methods

The **total carbon** (TC) and **total sulfur** (TS) content was determined using ELTRA instruments (CS 530; CS 500 TIC). The weighed and milled sample is heated in an O_2 atmosphere at ca. 1450 °C. All the carbon and sulfur in the sample is oxidized and converted to CO_2 and SO_2 gases, which are then detected in infrared cells. The **total inorganic carbon** (TIC) determination uses the same detection unit, but the sample is first treated in phosphoric acid (H_3PO_4), which leads to the selective transformation of C from carbonates into CO_2 being subsequently detected. The **total organic carbon** (TOC) is then calculated as the TC minus the IC.

The **Hg content** was determined using the CV-AAS method (cold vapor atomic absorption spectroscopy; Leco-Altec AMA 254). The sample is preheated in an O_2 atmosphere, the outcoming gases are filtered and the Hg is captured on an amalgamator. This approach enables one to separate the Hg from the matrix. The amalgamator is then heated, and all the Hg is evacuated into the measuring cells.

Inductively coupled plasma optical emission spectrometry (ICP-OES) uses ICP to produce excited atoms and ions that emit electromagnetic radiation at wavelengths characteristic of a particular element. An Agilent 5110 SVDV instrument was used to analyze the digests of our experimental samples and ashes.

Inductively coupled plasma mass spectrometry (ICP-MS) is a type of mass spectrometry, which uses inductively coupled plasma (ICP) to ionize elements from a liquid sample. The ions formed in the plasma are sorted by mass and detected with a high sensitivity. We used Thermo Scientific Plasma Quad II and iCAP™ instruments with a quadrupole and a Thermo Scientific Element 2™ with a magnet ion separation unit.

Box 4. Digestion of experimental samples and ashes

The weighed sample (0.2 g) was firstly treated in PTFE (polytetrafluorethylene) digestion vials with a mixture of HNO_3 (8 ml), H_2O_2 (30 µl) and HF (30 µl) (see figure below). This mixture was properly enclosed and heated up to 300 °C. In the second step, using deionized (DI) water, the suspension was transferred into centrifuging vials and centrifuged (4000 rpm for 5 min). Afterwards, the obtained liquid was diluted, and the solid residue was transferred back into PTFE vials and treated with $HClO_4$ (10 ml) and HF (0.5 ml) at ca. 170 °C. The digested residue was diluted with 5% HNO_3. By using this digestion protocol, we avoided applying direct heat to the sample during the ashing used in a conventional digestion procedure to obtain two liquids from each sample, which were analyzed using ICP-OES and ICP-MS. The validation of this digestion procedure was crosschecked using the certified reference materials reported in **Table 1**. This digestion procedure was found to be a good alternative to microwave-assisted digestion, especially for samples with a very high concentration of metal(loid)s.

Throughout the sample processing, certified reference materials and blank samples were simultaneously used. The experimental samples were highly complex and consisted of gangue/ore minerals, newly formed phases, variable slag phases, including glass of variable compositions, and organic

matter. Therefore, to check the accuracy of the digestion and subsequent analytical procedures, a combination of several certified reference materials with variable matrices was needed (**Table 1**). A satisfactory agreement between the measured and certified values was observed (for the complete datasets, see the Supplementary Materials of the papers attached as **Annexes I, II** and **III**).

Table 1. Certified reference materials used for the C, S, and metal(loid) measurements. More detailed information is given in the Supplementary Materials of **Annexes I** [1], **II** [2] and **III** [3].

Reference material	Characteristics	Element
[2]ELTRA 92510	Coal	C
[2]NIST 2701	Hexavalent Chromium in Contaminated Soil (High Level)	C_{inorg}
[2]NIST 2709	San Joaquin Soil	C, S
[2,3]NIST 1515	Apple Leaves	S, As, Cd, Cu, Fe, Pb, Zn
[2]NIST 1575	Pine Needles	S
[2]BCR 142R	Light Sandy Soil	Hg
[3]NIST 2711a	Montana Soil II	As, Cd, Cu, Fe, Pb, Zn
[3]NIST 1573a	Tomato Leaves	As, Cd, Cu, Fe, Pb, Zn
[3]Analytika Metranal™3	Strawberry Leaves	As, Cd, Cu, Fe, Pb, Zn
[1,3]CZN-4	Zinc Concentrate	As, Cd, Cu, Fe, Pb, Zn
[1,3]CCU-1e	Copper Concentrate	As, Cd, Cu, Fe, Pb, Zn

3.3 Mineralogical investigation

The experimental samples were first examined using optical microscopy. Concurrently, the selected biomass parts from each sample were adjusted on a carbon tape for further SEM/EDS investigations. Moreover, the heavy

mineral fractions of each soil (fraction <2 mm) or biomass sample were obtained using 1,1,2,2-tetrabromoethane (density 2.96 g/cm^3). The aliquot parts of both original samples and heavy mineral fractions were milled and used for the bulk chemical analyses and X-ray diffraction analysis (XRD). The aliquots of heavy mineral fractions were prepared as polished sections and were analyzed by scanning electron microscopy (SEM/EDS) and electron microprobe (EPMA) afterwards. The selected biomass fragments were also examined and analyzed using SEM/EDS to determine the shapes, sizes and chemical compositions of the particles adhering to the plant surfaces. Additionally, the soil heavy mineral fractions were studied using automated mineralogy (autoSEM). More detailed information about the equipment and measurements is given in **Boxes 5** and **6**.

Box 5. Mineralogical methods

An X-ray diffraction (XRD) analysis is a fundamental technique used for the identification of crystalline minerals/phases in a solid sample. This method is based on diffracting X-rays on a milled crystalline material in a defined (Bragg-Brentano) geometry and enables the phase recognition out of the obtained diffractograms, which were, in our case, processed using X'Pert HighScore Plus 3.0.3 software coupled with the Crystallography Open Database (COD). All the measurement were carried out by the PANalytical X'Pert Pro diffractometer (PANalytical, the Netherlands) equipped with an X'Celerator detector using CuK_{α} radiation at 40 kV and 30 mA over a range 2–80° 2theta (step 0.02°, counting time 150 s per step).

Scanning electron microscopy (SEM) uses an electron beam source to scan the sample surface (**SE** - secondary electrons) or acquire the image showing the relative atomic weight of the individual phases (**BSE** - back scattered electrons). Microscopes coupled with a Shottky cathode, also called a field emission gun (**FEG**), provide better resolution of the acquired image. An energy dispersive spectrometer (**EDS**) is used for the fast elemental analysis and relies on detection of X-ray spectra produced by an interaction of electrons with the sample.

Electron probe microanalysis (EPMA) is a non-destructive analytical method based on the detection of the specific X-ray wavelengths emitted from the analyzed sample in an instrument similar to the SEM. In contrast to EDS, wavelength dispersive X-ray spectroscopy (**WDS**) utilizes Bragg diffraction on crystals to select the specific X-ray wavelengths of interest and direct them to the detectors. Compared to EDS, it is a time-consuming detection method and provides data for just the selected element, but it is a more precise technique with lower detection limits.

To obtain electron micrographs and analyses for our experimental samples, we used an EPMA from JEOL (JXA-8530F, Japan) equipped with an FEG electron source, an EDS detector (JEOL JED-2300F) and five WDS spectrometers.

The description of the automated mineralogy (autoSEM) is given separately in Chapter 4 (**Box 6**).

3.4 Burning experiments

The Hg thermo-desorption (TD) experiments were conducted on the experimental samples using an AMA 254 CV-AAS, where the temperatures range of 75–670 °C was regulated using the software modification. An experimental sample was placed into a heating cell (quartz) throughout the experiment for all the temperature steps. At each temperature step, the Hg captured on the amalgamator was released and quantified according to the calibration common for bulk Hg measurements. The experiments were conducted under an O_2 gas flow to better simulate the wildfire conditions. Each TD curve was constructed from 16 data points. The TD experiment was conducted in three replicates for the experimental samples and the following reference compounds: Metranal®3 Strawberry Leaves reference material (Analytika Ltd., Czech Republic, representing the Hg bound to the organic matter, OM) and synthetic compounds such as metacinnabar (black HgS), cinnabar (red HgS), red HgO and Hg(II) adsorbed to goethite (FeOOH). Additionally, the experimental samples were also studied using thermogravimetry (TG; SDT 650, TA Instruments) to determine the temperature-related mass loss (25–1000 °C; step: 10 °C/min; air).

To simulate the potential wildfire effects on the topsoils under laboratory conditions, we introduced two novel experimental set-ups. A **single-step combustion experiment** (**Figure 7a**) was designed to simulate the wildfire conditions and consisted of a precise temperature setting, a continuous delivery of fresh air coupled with both a smoke outcome and the possibility of sampling the residual ash and emitted aerosols. The experiments were designed to decipher emissions at the temperature steps (250, 350, 450, 550, 650, 750 and 850 °C) covering a range of the topsoil heating levels that may occur during wildfires. During the burning procedure, a mass of 0.2 g of the homogenized topsoil sample was placed in a corundum boat and heated for 25 min in a pre-heated furnace (Clasic CZ, Czech Republic) equipped with a quartz tube. The burning experiments were conducted under synthetic air in order to closely simulate wildfire conditions and to ensure the repeatability of the experiment; the air supply was ca. 50 mL/min. For the selected runs, a PTFE filter assembly (porosity 1–2 μm, diameter 47 mm; both produced by Savillex®, USA) was placed at the outlet of the burning chamber to trap the aerosol particles for the additional mineralogical investigations. The final part of the setup consisted of a glass pipette for bubbling the outlet gas in the trapping solution (5% HNO_3) (**Figure 7a**). The obtained ashes (digested and analyzed using the same procedure as the original soil and biomass

samples, see above), trapping solutions, and solutions obtained by washing the set-up components (quartz tube and glass pipette; heated concentrated HNO_3) were all analyzed. For the metal(loid) mass balance calculations, the chemical compositions of the original soil and the obtained ash were used. Moreover, several mineralogical methods were used to investigate the ashes (XRD, FEG-SEM) and the aerosol particles trapped by the filtering unit (FEG-SEM).

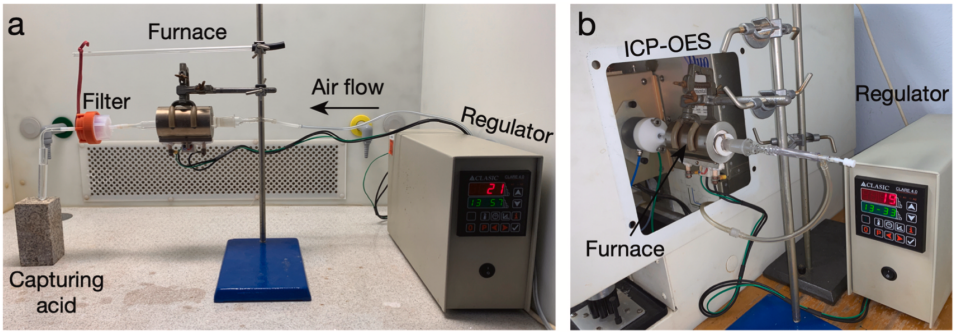

Figure 7. Laboratory wildfire simulation experimental set-ups. a) Single-step combustion set-up; b) Set-up with a continuous temperature increase and online detection.

The set-up with a continuous temperature increase and the online ICP-OES detection (**Figure 7b**) consisted of the combustion unit as in the already mentioned set-up (without the filter assembly) directly connected to the quartz injector of the ICP-OES plasma torch (at a distance of 5.5 cm). The sample was gradually heated from 25 °C

up to 750 °C for 14 min 30 s, applying a linear slope of 50 °C/min. The combustion products were directly introduced into the ICP-OES plasma employing an Ar stream (50 mL/min).

4 Solid speciation of metal(loid)s in soils

4.1 Conventional mineralogical methods

Detailed knowledge of the modal composition and element partitioning is essential for the solid interpretation of the wildfire effects on contaminated topsoils. Therefore, the samples were studied using conventional techniques such as optical microscopy, XRD and SEM/EDS (coupled with EPMA) to determine the contaminant-bearing phases.

All the heavy mineral fractions from the biomass-rich topsoils from Tsumeb (A, AM, G) were quite complex. Using XRD, we dominantly detected quartz (SiO_2), pyroxenes (diopside, $MgCaSi_2O_6$), olivine (fayalite, Fe_2SiO_4) and carbonates [dolomite, $(Ca,Mg)(CO_3)_2$] (more detailed information in the Supplementary Material, **Annex I**). They also contained significant amounts of amorphous compounds (e.g., slag glass), reflected in the diffractograms by an elevated background in the range of 15 and 40° 2theta. Besides the amorphous phases, all the samples were rich in other minor geogenic minerals and anthropogenic phases.

The commonly used approach for complex sample analysis by SEM is extremely time-consuming and generally, only up to a few hundred spot

analyses are collected (Knight and Henderson, 2006; Lanteigne et al., 2012; Ettler et al., 2016; Tyszka et al., 2016). Moreover, other limitations of this method are the operator's experience and preferences. As already mentioned by Pirrie and Rollinson (2011), the operator's eyes are usually attracted to high-density phases and might statistically overlook other phases important for the overall sample description.

4.2 Automated mineralogy (autoSEM)

Considering the above-mentioned limitations, we decided to quantitatively determine the contaminant partitioning by the automated mineralogy approach. A new generation of automated scanning electron microscopy (autoSEM) was used to study polished sections prepared from the heavy mineral fractions of the Tsumeb topsoils and was combined and optimized with conventional mineralogical techniques (SEM imaging with EDS analyses, 250 EPMA spot analyses) to increase the precision of the autoSEM calculations. Detailed information about the TESCAN Integrated Mineral Analyzer (TIMA) autoSEM measurements is given in **Box 6**. The accuracy of TIMA was checked by comparison of the bulk chemical analyses of the studied samples and the TIMA-calculated data. A good agreement between both methods was achieved.

Box 6. autoSEM

A TESCAN Integrated Mineral Analyzer (TIMA) (TESCAN VEGA3 GMH, Czech Republic) automated scanning electron microscopy (autoSEM) equipped with energy dispersion spectroscopy (EDS; 4 detectors PulseTor 30, USA) was used for the analysis of the modal compositions, the automated search and identification of metal(loid)-bearing phases and metal(loid) quantitative deportment. Using the TIMA software v1.6.68, the modal and textural analyses were performed using the specifically designed "dot mapping mode" called TIMA DotMapping (TDM) (Hrstka et al., 2018). This method combines a high-resolution (0.4 μm in our case) back-scattering electron (BSE) imaging and a lower resolution (2.5 μm in our case) EDS mapping. Between 29 and 75 million analyses were performed per sample (this corresponds to 33–72 thousand individual particles). The initial BSE scan is used to discriminate particles from the background (epoxy resin) and the grain borders between the individual phases in the heterogeneous particles. The "lower-resolution" EDS measurements/mapping provide additional elemental information for the phase identification of each segment and helps to detect different phases with the same BSE signal (for detailed parameters of the autoSEM measurements, see the Supplementary Material, **Annex I**).

4.3 Phase distribution

The quantitative phase distribution determination, including a large variety of particles of geogenic and anthropogenic origin, consists of tens of millions of spot analyses per sample. Hence, this is assumed to represent the volume % in the sample, even though it reflects the two-dimensional information. As shown in **Figure 8**, the resolution of the method is sufficient to even discriminate the submicrometric droplets (mainly Cu sulfides) and the surrounding matrix. The topsoils developed under *Acacia* spp. (sample A) and in the grassland (sample G) are similar in the modal phase composition, with the predominant slag glass (40.7–45.8 %), metal-rich Fe (oxyhydr)oxides (23–25.7 %) and calcite/dolomite (4.21–5.35 %). The proportion of the other phases in samples A and G is less than 4%. In contrast, sample AM is depleted in the slag glass (only 4.74%) and is mainly composed of Fe (oxyhydr)oxides (28.1 %), apatite group minerals (12.4 %) and calcite/dolomite (10.7 %) (**Annex I**). The unidentified/unsorted residue ranged from 5.90 to 9.24 %, which is relatively low in comparison with other studies (Pietranik et al., 2018).

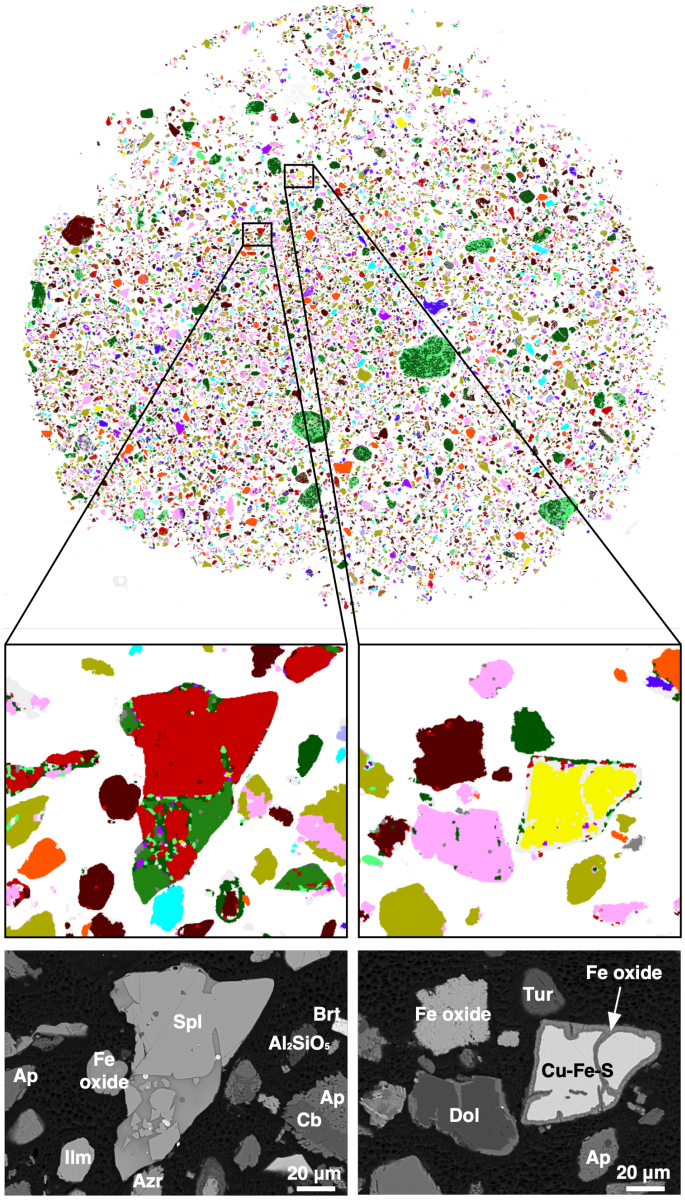

Figure 8. The autoSEM (TIMA) phase maps recorded in the heavy mineral fraction of a Tsumeb soil sample (AM) showing the high resolution of the method. Each pixel represents one EDS analysis. Abbreviations: Ilm - ilmenite ($FeTiO_3$), Azr - azurite [$Cu_3(CO_3)_2(OH)_2$], Ap - apatite [$Ca_5(PO_4)_3(F,Cl,OH)$], Brt - barite ($BaSO_4$), Cb - carbonate (variable composition), Dol - dolomite [$CaMg(CO_3)_2$], Spl - spinel (variable composition), Tur - tourmaline (variable composition) (modified from **Annex I**).

4.4 Deportment of metal(loid)s

The information about the metal(loid)s' partitioning within the individual phases (called deportment) is necessary to understand their potential remobilization during wildfire events. Using the autoSEM, it was possible to determine the deportment of the As, Cu, Pb and Zn (**Table 2**). We found that As was mainly bound to the apatite group minerals, slag glass and metal arsenates. Copper was predominantly hosted by the sulfides/sulfosalts and the Cu-bearing secondary carbonates. The deportment of Pb was relatively complex: slag glass, Fe and Mn (oxyhydr)oxides, metal arsenates/vanadates and cerussite were the most important carriers for Pb. Zinc was mainly bound to the slag glass, Fe (oxyhydr)oxides, smithsonite and sphalerite. In the case of Cd and Sb, the deportment could not be properly quantified due to their low concentrations in the experimental samples and spectral overlaps with some major elements (Sb vs. Ca, Cd vs. K and Ca in the studied soils). However, based on the test autoSEM measurements, we concluded that the Cd was mainly bound in arsenates, sulfides, slag glass and carbonates. More detailed information about the elemental partitioning is reported in Table 2 of **Annex I**.

Table 2. Metal(loid)-hosting phases in the experimental topsoils from Tsumeb (adapted from **Annex I**) (Abbreviations: HFO - hydrous ferric oxides).

Element	Sample	Phase
As	A	apatite, slag glass, arsenates
	AM	slag glass, HFO, duftite
	G	apatite, arsenates, duftite
Cu	A	sulfides, azurite/malachite, slag glass
	AM	azurite/malachite, sulfides, mottramite
	G	sulfides, sulfosalts, azurite/malachite
Pb	A	slag glass, HFO, cerussite
	AM	cerussite, mottramite, slag glass
	G	slag glass, HFO, sulfides
Zn	A	slag glass, HFO, smithsonite
	AM	HFO, slag glass, calcite, dolomite
	G	slag glass, HFO, smithsonite

Despite the many limitations of the method listed in **Annex I**, the autoSEM proved to be a convenient tool for a quantitative mineralogical/geochemical characterization of highly complex contaminated topsoil samples. Its outcomes substantially helped to interpret the metal(loid)s' fate during wildfires.

5 Hg emissions during combustion

Wildfires cause significant Hg emissions into the atmosphere (Wiedinmeyer and Friedli, 2007; Navrátil et al., 2009; Campos et al., 2015). We investigated the Hg distribution in the topsoil and vegetation samples and the thermo-desorption (TD) of Hg from the experimental topsoils collected near a Cu smelter in Tsumeb (Namibia). These topsoils exhibited very high Hg concentrations (3.9–7.7 mg/kg) due to emissions from the metallurgical processing of Hg-rich Cu concentrates (at the time of sampling, mainly originating from Bulgaria and Chile, Hg concentrations: 20.7–39.9 mg/kg).

To clearly determine the source of the remobilized Hg during the wildfire-simulating experiments, knowledge of the Hg speciation is of key importance. Unfortunately, no specific Hg-bearing phases were detected in the experimental samples using conventional mineralogical methods. Therefore, the X-ray absorption spectrometry (XAS) measurements, namely X-ray absorption near-edge structure (XANES) and the extended X-ray absorption fine structure (EXAFS) spectra of the powdered samples, were collected at the SUL-X beamline at the Angströmquelle Karlsruhe (ANKA, Eggenstein-Leopoldshafen, Germany). Despite numerous

attempts to optimize the XAS measurements, the resulting data did not yield the desired information about the Hg speciation in our experimental topsoils and technological samples. The concentration of Hg in the samples was found to be relatively low for this method. Additionally, μ-XRF spectroscopy was used on the polished sections prepared for the experimental samples to check the sample homogeneity and verify the potential presence of the Hg-rich hotspots. The μ-XRF measurements indicated that the Hg distribution was quite homogeneous, which prevents the application of EPMA/μ-XANES/μ-EXAFS to determine the Hg speciation (more detailed information about the used methods is given in the Supplementary Material of **Annex II**). Based on this information, we decided to perform the TD experiments on a variety of laboratory-prepared reference compounds, technological samples from the Tsumeb ore processing circuit to decipher the source of the Hg contamination in the local topsoils.

Both the total Hg total concentrations and TD analyses were carried out using an AMA 254 instrument (see **Box 3;** in the case of the TD, with software modifications). The TD outputs were supported by the TG measurements. The dominant weight loss at temperatures >300 °C corresponds to the major Hg emission. This might be related

to the combustion processes under the oxygen-rich atmosphere. Nevertheless, the same TD results were obtained under the N_2-atmosphere and confirmed that, in this case, the Hg release is not influenced by the O_2-driven uncontrolled biomass burning in the instrument furnace (Supplementary Information of **Annex II**).

5.1 Mercury distribution in topsoils

Mercury in the vegetation samples collected around the Tsumeb site is significantly lower (0.00297–0.186 mg/g; n = 28) than in the topsoils (0.0233–3.79 mg/g; n = 30). The Hg spatial distribution patterns indicated that the prevailing wind direction has a significant role in the Hg transport (**Figure 9**). Nevertheless, the shape of the Hg hotspot in the topsoils is less elongated likely due to the limited transport distance of the particles from the smelter and the nearby disposal sites. In contrast, the Hg in the vegetation probably reflects the ability of the plants to uptake the gaseous Hg (Lodenius et al., 2003; Millhollen et al., 2006), which can be transported over larger distances from the source (Wu et al., 2014; Yin et al., 2009).

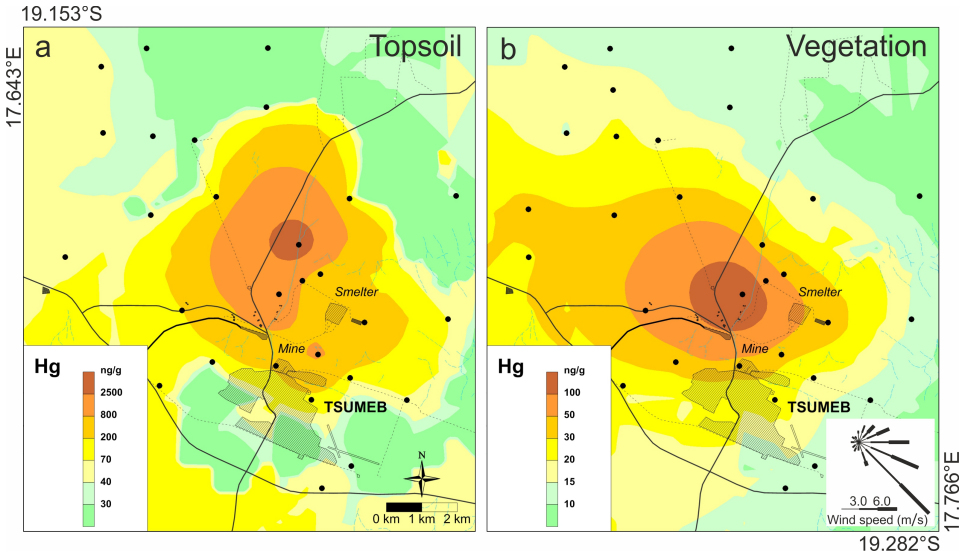

Figure 9. Mercury distribution maps in the topsoil (a) and vegetation (b) in the sampling area of the Tsumeb smelter (Namibia). The sampling sites are marked as black dots (adapted from **Annex II**).

5.2 Mercury remobilization during a simulated wildfire

All the experimental samples exhibited the same TD peak at ~340 °C, which corresponded to more than 91 % of total Hg remobilized (**Figure 10a**). When compared to the TD curves of the technological samples (**Figure 10b**) and reference compounds (**Figure 10c**), it can be hypothesized that the Hg in the experimental samples occurs as a mixture of Hg bound to the organic matter and metacinnabar (black HgS), which presumably originates from the flue gas stream in the smelter (Kim et al., 2004). We assume that the metacinnabar in the experimental topsoils are probably associated with nm-sized particulates because

no distinct Hg-bearing particles were found by any of the used imaging techniques (SEM, μ-XRF).

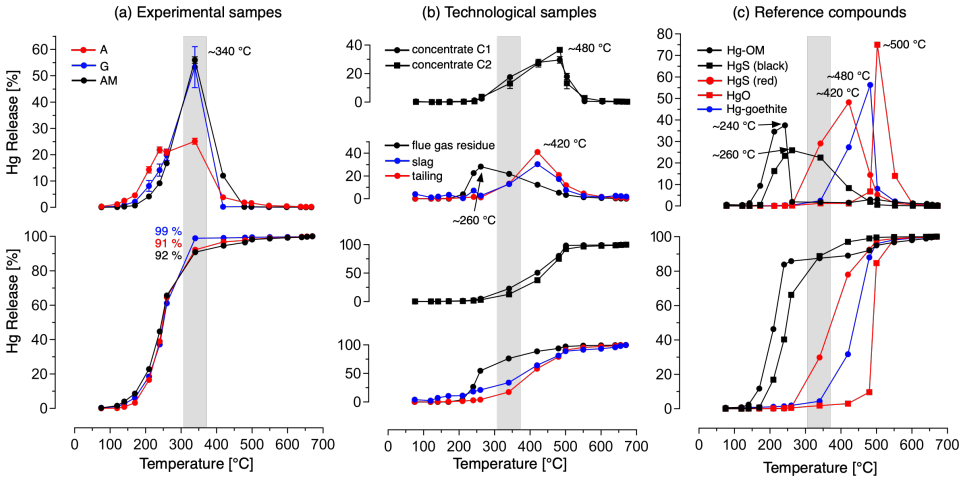

Figure 10. Mercury TD curves for (a) the biomass-rich topsoils (experimental samples), (b) the technological samples (Cu concentrates, flue gas residue, slag, tailing) and (c) the reference compounds indicating a temperature-dependent Hg release (adapted from **Annex II**).

5.3 Estimations of potential Hg remobilization from polluted hotspots

Based on the acquired Hg distribution maps, we were able to estimate the worst-case scenario of the potential amount of Hg remobilized during the wildfires. Our calculations (given in **Annex II**) estimated that the remobilizable Hg for the entire studied area (vegetation: 0.07 g/ha, topsoil: 16.45 g/ha) is in the same order of magnitude as those at other sites (Europe: 1.1-75.1 g/ha; North America: 0.36-30 g/ha) (Campos

et al., 2015; Engle et al., 2006; Navrátil et al., 2009; Webster et al., 2016). However, the remobilizable Hg in the polluted hotspots is much higher and corresponds to 0.5 g Hg/ha for the vegetation and 229 g Hg/ha for the topsoil. Thus, our spatial distribution data in the contaminated surroundings of the Tsumeb smelter indicate that ~300 kg Hg can be remobilized by a wildfire from the whole area with a surface of 184 km^2.

6 Wildfire driven metal(loid) emissions from the topsoil and biomass

6.1 Temperature-dependent release of metal(loid)s from topsoils

Single-step combustion experiments combined with the experiments performed using the set-up with the online ICP-OES detection (described in **Chapter 3.4**) indicated that the metals (Cd, Cu, Pb and Zn) were dominantly concentrated in the ash residue at temperatures <550 °C. If exposed to higher temperatures, the metals were partially released (above 550–600 °C, **Figure 11**). Under this temperature exposure, the aerosol slag-like particles enriched in the metals were emitted. The presence of such particles trapped on filters using the filtration assembly of the single-step combustion setup was confirmed by the subsequent analyses (EDS/SEM) (**Figure 12**).

Arsenic behavior during wildfires is substantially more complicated (**Figure 11**), due to the complexity of As solid-state speciation in the samples (**Annex I**). The main peaks of As emissions were observed at the temperatures of 275 °C, 370–410 °C and 580 °C. Combining the experimental results and the data from the literature (e.g., Johnston et al., 2018, 2019), we hypothesized that As is successively released

from As-bearing hydrous ferric oxides at temperature ~275 °C. The multiple peaks of As emissions in the temperature range of 370–410 °C likely correspond to the complex decomposition of the various As-containing phases (arsenolite, arsenates and As-bearing apatite) attached to the organic matter fragments present in the soil litter (**Figure 13b, d**). A sharp As emission at 580 °C most likely corresponds to the decomposition of enargite (Cu_3AsS_4) (Safarzadeh and Miller, 2016), which is also supported by the concurrent release of sulfur (~600 °C, **Annex III**).

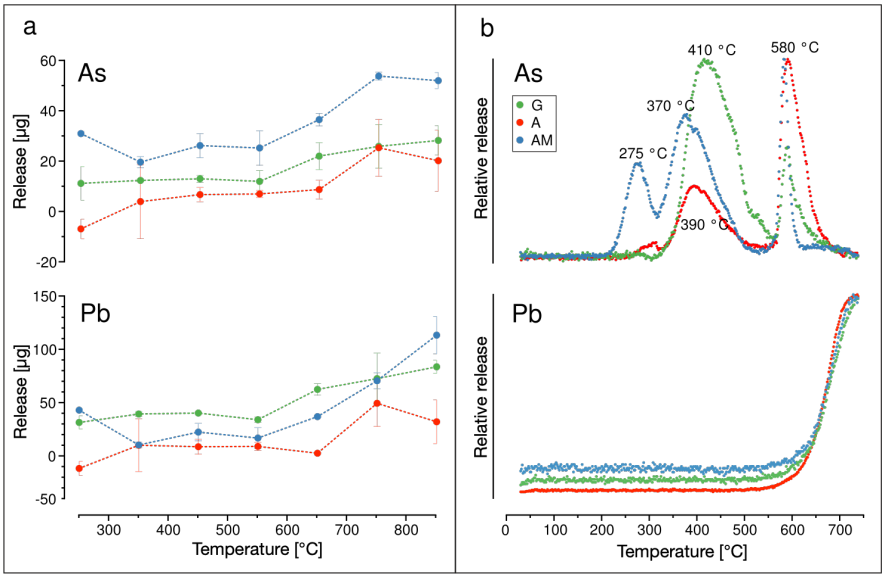

Figure 11. a) Amounts of the As and Pb released from the heated experimental topsoils (in µg; initial sample mass: 0.2 g) as a function of the temperature as obtained by the single-step combustion set-up. The trend lines were drawn to guide the eyes. The positive values correspond to the release, and the negative values and their standard deviations correspond to the accumulation of a given element; b) Relative release of As and Pb as obtained by the wildfire-simulating set-up with a continuous temperature increase and online measurement. The experimental topsoil samples were collected under the acacia trees (A), acacia and marula trees (AM) and in a grassland (G).

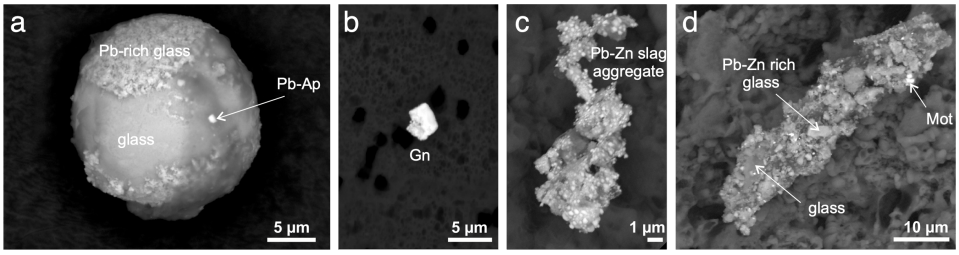

Figure 12. FEG-SEM micrographs of the particles emitted during the wildfire-simulating experiments conducted on the Tsumeb topsoils and trapped by the filtering unit (see **Figure 8a**). a) Spherical slag-like aerosol particle with anattached submicrometric grain of Pb-bearing apatite; b) Minute grain of galena (Gn, PbS); c) Aggregate of small Pb- and Zn-bearing slag particles; d) Aggregate of various Pb-Zn-bearing slag glass particles with attached mottramite-like grains [Mot, $PbCu(VO_4)(OH)$].

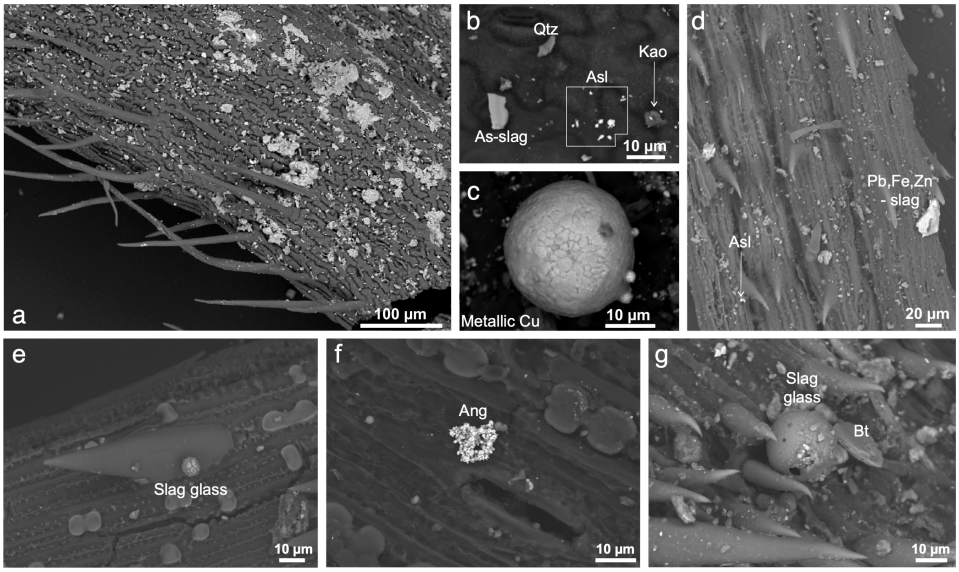

Figure 13. FEG-SEM micrographs in back-scattered electrons (BSE) of the particles adhering to the surfaces of the biomass fragments from the experimental topsoil samples (Tsumeb, Namibia a-d; adapted from **Annex III**) and vegetation samples (e-g; grass; adapted from **Figure AVI-2** of **Annex IV**); a) Plant fragment covered with the windblown dust particles; b) Geogenic (quartz, kaolinite) and smelter-derived particles (As-slag, arsenolite) attached to the vegetation surface; c) Smelter-emitted spherical Cu metal particle; d) Fragment of grass with attached arsenolite and metal-bearing slag particles; e) Spherical slag glass particle (Selebi-Phikwe, Botswana); f) Newly formed microcrystalline anglesite (Kabwe, Zambia); g) Slag glass particle in association with biotite (Luanshya, Zambia). Abbreviations: Ang – anglesite ($PbSO_4$); Asl – arsenolite (As_2O_3); Bt – biotite [$K(Mg,Fe^{2+})_3[(OH,F)_2(Al,Fe^{3+})Si_3O_{10}]$]; Kao – kaolinite [$Al_2Si_2O_5(OH)_4$]; Qtz – quartz ($SiO_2$)

6.2 Temperature-dependent release of metal(loid)s from grass/biomass

The surfaces of all the grass biomass samples contained a variety of geogenic (quartz, carbonates, clay minerals) and anthropogenic (usually metal-bearing) particles. These smelter-derived particles are predominantly slag fragments enriched in various contaminants, droplets

of metals/sulfides, and, in the case of the biomass from Kabwe, newly formed aggregates of submicrometric anglesite ($PbSO_4$) (**Figure 13e-g**).

The wildfire-simulating experiments using the single-step combustion set-up were performed at 250 °C, 550 °C and 850 °C in three replicates to simulate all types of wildfire intensity. Even though the grass samples were not finely milled, but just disaggregated in a cutting machine, the comparison of the weight losses in the individual replicates proved very low experimental errors (**Figure AIV-3** of **Annex IV**). The colors of the obtained ashes indicated substantial changes as a function of the temperature. Úbeda et al. (2009) observed that the ash color during the combustion of cork oak litter (*Quercus suber*) is yellowish at <150 °C (loss of water), reddish at 200–250 °C (oxidation of Fe-bearing minerals), black at 300 °C (forming of black carbon), and gray/white at >400 °C (newly formed $CaCO_3$). Compared to this observation, the ashes from our samples T and L were paler at every temperature step. In contrast, sample SP was slightly darker at a temperature of 850 °C when compared to 550 °C and sample K was black even at a temperature of 850 °C (**Figure AIV-4** of **Annex IV**). This possibly indicates that the color of the residual ash may be influenced by many variables, such as the original composition of the sample (geochemical, mineralogical), the temperature gradient

and time of exposure. It is nevertheless important to stress that the collected ashes have not been sufficiently analyzed yet and definitely need further investigation (e.g., FEG-SEM, XRD). As mentioned by Bento-Gonçalves (2012), wildfire-generated ashes might be used for the further determination of a fire's severity only when compared with laboratory-prepared ash standards.

Wildfire-simulating experiments on grass/biomass samples have not been sufficiently interpreted yet. In some cases, the mass-balance calculations were not clear and indicated the inexplicable metal(loid)s enrichment of the ash. We are aware of the need for further additional data processing, especially by using advance statistical data treatment considering all the possible errors generated by both the experimental protocol (e.g., inhomogeneity of the samples) and the analyses of the obtained ashes. Nevertheless, the obtained dataset indicates that, during biomass combustion, metals are most probably concentrating in the ash residue (**Annex IV**).

6.3 Potential metal(loid) releases during wildfires

The temperature of 850 °C was used in our experiments as a "worst-case scenario" that can occur during the heating of biomass-rich topsoils. At this temperature, the contaminants' releases were calculated as a percentage of the totals, finally corresponding to 5–14 % As, 2–12 % Cu, 100 % Hg, 3–17 % Pb, 2–20 % Zn and 27–79 % Cd, which are not negligible (note that for Cd, the total concentrations are significantly lower compared to the other metal(loid)s) (**Annex III**). These values just serve as estimations based on the samples collected close to the Tsumeb smelter in the semi-arid north of Namibia. Despite the fact that the sampling was performed in a relatively small area, the samples exhibited substantial variation in the concentrations/partitioning of the contaminants and mineralogical composition. Therefore, using these data is quite limited for further extrapolation and regional/global estimates.

7 Environmental implications, outlook, and future work

Contamination hotspots near metal mines and smelters in areas exposed to frequent wildfires (e.g., Australia, the Americas, Siberia, southern Africa) may be a significant source of metal(loid) remobilization (Mihaljevič et al., 2011; Ettler et al., 2014; Abraham et al., 2018b). Determination of the contaminants' emissions during wildfires and transformations of the burned materials at polluted sites may be complicated due to the high complexity of the metal(loid) speciation. We tried to overcome these difficulties by firstly analyzing the samples using TIMA (autoSEM). Even though this technique is conventionally used in the mining industry, after optimization, it helped to interpret the modal phase distribution as well as the contaminant partitioning and textural relations. Nonetheless, we still face many difficulties. Coupling the sample complexity and variability within a small distance at the given locality significantly complicates the overall estimations of the metal(loid)s' fate. Moreover, the occurrence of wildfires in savannas is often patchy, so the prediction of potential local-to-regional remobilizations and fluxes of metal(loid)s is difficult. When comparing the time of the data acquisition and the number of analyses, the autoSEM technique is relatively fast,

but still not applicable with hundreds of samples, mainly due to its price and processing-time requirements. Another problem arises with the setting of boundaries in the individual phases, where substitutions might occur; in this case, this was cross-checked by quantitative EPMA analyses acquired on a specific sample to optimize the autoSEM database. This step is also time-consuming. It is important to state that the heavy mineral fraction of the topsoils accounted for 4.31 ± 1.81 % of the total mass. However, when the amounts of metal(loid)s bound to the heavy mineral fractions were calculated, they corresponded to 24.3 ± 8.44 % of the total content in the topsoil (median: 21.5 %), which is a relatively low amount when compared with the total metal(loid) contents in the samples. This suggests that the metal(loid)s are also bound to a less dense soil fraction, such as metal(loid)-bearing phases embedded/locked in larger crystals of quartz, calcite and other geogenic minerals. Additionally, contaminant-bearing particles might be attached to the plant surfaces (e.g., leaf cuticle) in the form of (nano)particles (Kříbek et al., 2014, 2016, 2018; Uzu et al., 2009) or absorbed by the plants' roots (Kříbek et al., 2014; Mihaljevič et al., 2015; Uzu et al., 2009). As a result, autoSEM is a valid tool for mineralogical/geochemical analyses of contaminated sites, but must be supported with other analytical techniques. For example, any future investigation might be improved by concurrent (μ)XAS

measurements. Our μXRF mapping of the polished sections prepared from the topsoil biomass fragments indicated that Hg was evenly distributed, but other contaminants formed hotspots, which could potentially be analyzed by (μ)XAS. For the mass-balance calculations and estimations for the emissions from larger areas, a detailed investigation of the contaminants' speciation should be performed on a much larger number of samples covering both the contaminated sites and remote areas.

The thermal stabilities and related element emissions during the simulated wildfires have not been determined for many of the metal(loid)-hosting minerals and phases. To better interpret the temperature-dependent release patterns, similar experiments should be performed on pure metal(loid)-bearing phases (selected minerals/phases, synthetic analogs) or a mixture thereof with a lab-prepared soil (uncontaminated soil), inspired by previous studies on the thermal alteration of As-bearing Fe oxides (Johnston et al., 2016, 2018, 2019). Further experimentation is needed to understand the nature of aerosols and gaseous emissions from these burned topsoils/biomass samples to better quantify the wildfire-induced fluxes of the individual elements and to improve the mass-balance calculations. Moreover, as suggested by Wienhold (2011), investigation of human health

effects of wildfire-emitted contaminants should be carried out especially in polluted areas.

This Ph.D. thesis raises many other questions: (i) If (and how) lab-scale burning experiments can be extrapolated to real-scale conditions given the spatial variability in the vegetation cover and the soil composition (e.g., complexity in the partitioning of the contaminants). (ii) How to design the *in situ* burning experiments to overcome all the mentioned difficulties.

The most appropriate simulation of wildfires should be based on *in situ* experiments. An experimental field should cover the representative area and must be appropriately equipped with thermocouples, aerosol samplers, and cameras. Such experiments are, of course, very expensive and must be supervised by experts to avoid the unwanted spread of a fire into the surroundings. The Pyrotron facility (mentioned in Chapter 2.2) might be a good compromise between the *in situ* experiments and the laboratory methods. Compared to other so-called 'burning benches', Pyrotron is already equipped with a variety of sensors to simultaneously control the airflow, to sample the aerosols, to register the temperature online, and to record the video in several modes (HD,

high speed, high resolution infrared thermal imaging) (https://www.csiro.au/en/work-with-us/use-our-labs-facilities/pyrotron-facility). The maximum capacity of 15 kg of dry fuel seems to be sufficient to simulate the real wildfire conditions more closely on a larger scale and might help to better estimate the metal(loid) fluxes during wildfires.

To conclude, the presented lab-scale experimental set-up offers several advantages of single wildfire-simulations. These include (i) the possibility of sampling the ashes, (ii) trapping the aerosols and outcoming gases, and (iii) the possible "online" detection of the emitted contaminants as a function of temperature. Also, it overcomes the limitations of wildfire simulations previously performed in muffle furnaces, because it enables a continuous airflow throughout the whole setup and better simulates the natural conditions (see also the limitations mentioned by Bryant et al., 2005). Nevertheless, this experimental approach cannot currently serve as a tool for estimating large-scale emission scenarios, but might be beneficial for local studies and understanding the individual processes driving the wildfire-induced remobilizations of metal(loid)s.

8 References

Abraham, J., Dowling, K., Florentine, S., 2017. Risk of post-fire metal mobilization into surface water resources: A review. Sci. Total Environ. 599-600: 1740-1755. https://doi.org/10.1016/j.scitotenv.2017.05.096

Abraham, J., Dowling, K., Florentine, S., 2018a. Effects of prescribed fire and post-fire rainfall on mercury mobilization and subsequent contamination assessment in a legacy mine site in Victoria, Australia. Chemosphere 190: 144-153. https://doi.org/10.1016/j.chemosphere.2017.09.117

Abraham, J., Dowling, K., Florentine, S., 2018b. Influence of controlled burning on the mobility and temporal variations of potentially toxic metals (PTMs) in the soils of a legacy gold mine site in Central Victoria, Australia. Geoderma 331: 1–14. https://doi.org/10.1016/j.geoderma.2018.06.010

Araya, S.N., Meding, M., Berhe, A.A., 2016. Thermal alteration of soil physico-chemical properties: a systematic study to infer response of Sierra Nevada climosequence soils to forest fires. Soil 2: 351-356. https://doi.org/10.5194/soil-2-351-2016

Aznar, J., González-Pérez, J.A., Badía, D., Marti, C., 2016. At what depth are the properties of a gypseous forest topsoil affected by burning? Land Degrad. Dev. 27: 1344-1353. https://doi.org/10.1002/1dr.2258

Badía-Villas, D., Gonzáles-Pérez, J.A., Aznar, J.M., Arjona-García, B., Marti-Dalmau, C., 2014. Changes in water repellency, aggregation and organic matter of a mollic horizon burned in laboratory: Soil depth affected by fire. Geoderma 213: 400-407. https://doi.org/j.geoderma.2013.08.038

Beale, C.M., Mustaphi, C.J.C., Morrison, T.A., Archibald, S., Anderson, T.M., Dobson, A.P., Donaldson, J.E., Hempson, G.P., Probert, J., Parr, C.L., 2018. Pyrodiversity interacts with rainfall to

increase bird and mammal richness in African savannas. Ecol. Lett. 21: 557-567. https://doi.org/10.1111/ele.12921

Beavington, F., Cawse, P.A., Wakenshaw, A., 2004. Comparative studies of atmospheric trace elements: improvements in air quality near copper smelter. Sci. Total Environ. 332: 39-49. https://doi.org/10.1016/j.scitotenv.2004.04.016

Bento-Gonçalves, A., Vieira, A., Úbeda, X., Martin, D., 2012. Fire and soils: Key concepts and recent advances. Geoderma 191: 3-13. https://doi.org/10.1016/j.geoderma.2012.01.004

Bryant, R., Doer, S.H., Helbig, M., 2005. Effect of oxygen deprivation on soil hydrophobicity during heating. Int. J. Wildland Fire 14: 449–455. https://doi.org/10.1071/WF05035

Butz, R.J., 2009. Traditional fire management: historical fire regimes and land use change in pastoral East Africa. Int. J. Wildland Fire 18: 442-450. https://doi.org/10.1071/WF07067

Campos, I., Abrantes, N., Keizer, J.J., Vale, C., Pereira, P., 2016. Major and trace elements in soils and ashes of eucalypt and pine forest plantation in Portugal following a wildfire. Sci. Total Environ. 572: 1363-1376. https://doi.org/10.1016/j.scitotenv.2016.01.190

Campos, I., Vale, C., Abrantes, N., Keizer, J.J., Pereira, P., 2015. Effect of wildfire on mercury mobilization in eucalypt and pine forests. Catena 131: 149-159. https://doi.org/10.1016/j.catena.2015.02.024

Cancelo-Gonzáles, J., Cachaldora, C., Díaz-Fierros, F., Prieto, B., 2014. Colorimetric variations in burnt granitic soils in relation to fire severity. Ecol. Indic. 46: 92-100. https://doi.org/10.1016/j.ecolind.2014.05.037

Cawson, J.G., Nyman, P., Smith, H.G., Lane, P.N.J., Sheridan, G.J., 2016. How soil temperatures during prescribed burning affect soil water repellency, infiltration and erosion. Geoderma 278: 12-22. http://dx.doi.org/10.1016/j.geoderma.2016.05.002

Crisp, M.D., Burrows, G.E., Cook, L.G., Thornhill, A.H., Bowman, D.M.J.S., 2010. Flammable biomes dominated by eucalypts originated at the Cretaceous-Paleogene boundary. Nat. Commun. 2: 193. https://doi.org/10.1038/ncomms1191

CSIRO, Pyrotron: A National bushfire research facility, accessed on 10.5.2021, https://www.csiro.au/en/work-with-us/use-our-labs-facilities/pyrotron-facility

CSIRO, Science Image, accessed on 11.5.2021, https://www.scienceimage.csiro.au/mediarelease/mr08-216.html

Dundee Precious Metals, accessed on 1.5.2021, https://www.dundeeprecious.com

Engle, M.A., Gustin, M.S., Johnson, D.W., Murphy, J.F., Miller, W.W., Walker, R.F., Wright, J., Markee, M., 2006. Mercury distribution in two Sierran forest and one desert sagebrush steppe ecosystems and the effects of fire. Sci. Total Environ. 367: 222e233. https://doi.org/10.1016/j.scitotenv.2005.11.025

Ettler, V., 2016. Soil contamination near non-ferrous metal smelters: A review. Appl. Geochem. 64: 56-74. https://doi.org/10.1016/j.apgeochem.2015.09.020

Ettler, V., Johan, Z., Kříbek, B., Veselovský, F., Mihaljevič, M., Vaněk, A., Penížek, V., Majer, V., Sracek, O., Mapani, B., Kamona, F., Nyambe, I., 2016. Composition and fate of mine- and smelter-derived particles in soils of humid subtropical and hot semi-arid areas. Sci. Total Environ. 563–564: 329–339. https://doi.org/10.1016/j.scitotenv.2016.04.133

Ettler, V., Konečný, L., Kovářová, L., Mihaljevič, M., Šebek, O., Kříbek, B., Majer, V., Veselovský, F., Penížek, V., Vaněk, A., Nyambe, I., 2014. Surprisingly contrasting metals distribution and fractionation patterns in copper smelter-affected tropical soils in forested and grassland areas (Mufulira, Zambian Copperbelt). Sci. Total Environ. 473–474: 117–124. https://doi.org/10.1016/j.scitotenv.2013.11.146

Ettler, V., Mihaljevič, M., Kříbek, B., Majer, V., Šebek, O., 2011. Tracing the spatial distribution and mobility of metal/metalloid contaminants in oxisols in the vicinity of the Nkana copper smelter, Copperbelt province, Zambia. Geoderma 164: 74-84. https://doi.org/10.1016/j.geoderma.2011.05.014

Gaudichet, A., Echalar, F., Chatenet, B., Quisefit, J.P., Malingre, G., Cachier, H., Buat-Menard, P., Artaxo, P., Maenhaut, W., 1995. Trace elements in tropical African savanna biomass burning aerosols. J. Atmos. Chem. 22: 19-39. https://doi.org/10.1007/BF00708179

Google Maps, accessed on 23.1.2020, https://bit.ly/3dj3x94

Gould, J.S., Sullivan, A.L., Hurley, R., Koul, V., 2017. Comparison of three methods to quantify the fire spread rate in laboratory experiments. Int. J. Wildland Fire 26: 877-883. https://doi.org/10.1071/WF17038

Harari, Y.N., 2015. Sapiens: A Brief History of Humankind. New York: Harper Perennial. ISBN: 9780062316097

Harvey, P.J., Rouillon, M., Dong, C., Ettler, V., Handley, H.K., Taylor, M.P., Tyson, E., Tennant, P., Telfer, V., Trinh, R., 2017. Geochemical sources, forms and phases of soil contamination in an industrial city. Sci. Total Environ. 584-585: 505-514, http://dx.doi.org/10.1016/j.scitotenv.2017.01.053

Hassan, S. N., Rusch, G. M., Hytteborn, H., Skarpe, C., & Kikula, I., 2008. Effects of fire on sward structure and grazing in western Serengeti, Tanzania. Afr. J. Ecol. 46(2): 174–185. https://doi.org/10.1111/j.1365-2028.2007.00831.x

Hou, X., Parent, M., Savard, M.M., Tasse, N., Bégin, C., Marion, J., 2006. Lead concentrations and isotope ratios in the exchangeable fraction: tracing soil contamination near a copper smelter. Geochemistry: Exploration, Environment, Analysis 6: 229-236. https://doi.org/10.1144/1467-7873/05-092

Howard, D., Macsween, K., Edwards, G.C., Desservettaz, M., Guérette, E.-A., Paton-Walsh, C., Surawski, N.C., Sullivan, A.L., Weston, C., Volkova, L., Powell, J., Keywood, M.D., Reisen, F., Meyer, C.P.M., 2019. Investigation of mercury emissions from burning of Australian eucalypt forest surface fuels using a combustion wind tunnel and field observations. Atmos. Environ. 202: 17-27. https://doi.org/10.1016/j.atmosenv.2018.12.015

Hrstka, T., Gottlieb, P., Skála, R., Breiter, K., Motl, D., 2018. Automated mineralogy and petrology e applications of TESCAN integrated mineral analyzer (TIMA). J. Geosci. 63: 47e63. https://doi.org/10.3190/jgeosci.250

Isley, C.F., Taylor, M.P., 2020. Atmospheric remobilization of natural and anthropogenic contaminants during wildfires. Environ. Pollut. 267: 115400. https://doi.org/10.1016/j.envpol.2020.115400

Jahn, L.G., Jahl, L.G., Bland, G.D., Monroe, L.W., Sullivan, R.C., 2021. Metallic and crustal elements in biomass-burning aerosol and ash: Prevalence, significance, and similarity to soil particles. ACS Earth Space Chem. 5: 136-148. https://doi.org/10.1021/acsearthspacechem.0c00191

Johnston, S.G., Karimian, N., Burton, E.D., 2019. Fire promotes arsenic mobilization and rapid arsenic(III) formation in soil via thermal alteration of arsenic-bearing iron oxides. Front. Earth Sci. 7: 139. https://doi.org/10.3389/feart.2019.00139

Johnston, S.G., Bennett, W.W., Burton, E.D., Hockmann, K., Dawson, N., Karimian, N., 2018. Rapid arsenic(V)-reduction by fire in schwertmannite-rich soil enhances arsenic mobilization. Geochem. Cosmochim. Acta 227: 1–18. https://doi.org/10.1016/j.gca.2018.01.031

Johnston, S.G., Burton, E.D., Moon, E.M., 2016. Arsenic mobilization is enhanced by thermal transformation of schwertmannite. Environ. Sci. Technol. 50: 8010–8019. https://doi.org/10.1021/acs.est.6b02618

Jones, J.C, Raj, S.C., 1988. The self-hearing and ignition of vegetation debris. Fuel 67: 1208-1210. https://doi.org/10.1016/0016-2361(88)90039-7

Jordan, P., 2016. Post-wildfire debris flows in southern British Columbia, Canada. Int. J. Wildland Fire 25: 322-336. https://doi.org/10.1071/WF14070

Kamona, A.F., Friedrich, G.H., 2007. Geology, mineralogy and stable isotope geochemistry of the Kabwe carbonate-hosted Pb-Zn deposit, Central Zambia. Ore Geol. Rev. 30: 217–243. https://doi.org/10.1016/j.oregeorev.2006.02.003

Kamona, A.F., Nyambe, I.A., 2002. Geological characteristics and genesis of stratiform sediment-hosted Cu-(Co) deposits, Zambian Copperbelt, In: Proceedings of the 11th IAGOD Quadrennial Symposium and Geocongress, Extended Abstracts (R.E. Miller, editor), Geological Survey of Namibia, Windhoek, Namibia

Kayee, J., Sompongchaiyakul, P., Sanwlani, N., Bureekul, S., Wang, X., Das, R., 2020. Metal concentrations and source apportionment of $PM_{2.5}$ in Chiang Rai and Bangkok, Thailand during a biomass burning season. ACS Earth Space Chem. 4: 1213-1226. https://doi.org/10.1021/acsearthspacechem.0c00140

Keeley, J.E., 2009. Fire intensity, fire severity, and burn severity: a brief review and suggested usage. Int. J. Wildland Fire 18: 116-126. https://doi.org/10.1071/WF07049

Kim, C.S., Rytuba, J.J., Brown Jr., G.E., 2004. Geological and anthropogenic factors influencing mercury speciation in mine waste: an EXAFS spectroscopy study. Appl. Geochem. 19: 379e393. https://doi.org/10.1016/S0883-2927(03)00147-1

Knight, R.D., Henderson, P.J., 2006. Smelter dust in humus around Rouyn-Noranda. Québec. Geochem.-Explor. Environ. Anal.6: 203-214. https://doi.org/10.1144/1467-7873/05-087

Kříbek, B., Majer, V., Knésl, I., Keder, J., Mapani, B., Kamona, F., Mihaljevič, M., Ettler, V., Penížek, V., Vaněk, A., Šráček, O., 2016.

Contamination of soil and grass in the Tsumeb smelter area, Namibia: modeling of contaminants dispersion and ground geochemical verification. Appl. Geochem. 64: 75e91. https://doi.org/10.1016/j.apgeochem.2015.07.006

Kříbek, B., Majer, V., Knésl, I., Nyambe, I., Mihaljevič, M., Ettler, V., Sracek, O., 2014. Concentrations of arsenic, copper, cobalt, lead and zinc in cassava (Manihot esculenta Crantz) growing on uncontaminated and contaminated soils of the Zambian Copperbelt. J. Afr. Earth Sci. 99: 713e723. https://doi.org/10.1016/j.jafrearsci.2014.02.009

Kříbek, B., Majer, V., Veselovský, F., Nyambe, I., 2010. Discrimination of lithogenic and anthropogenic sources of metals and sulphur in soils of the central-northern part of the Zambian Copperbelt Mining District: A topsoil vs. subsurface soil concept. J. Geochem. Explor. 104: 69-86. https://doi.org/10.1016/j.gexplo.2009.12.005

Kristensen, L.J., Taylor, M.P., Flegal, A.R., 2017. An odyssey of environmental pollution: The rise, fall and remobilisation of industrial lead in Australia. Appl. Geochem. 83: 3-13. https://doi.org/10.1016/j.apgeochem.2017.02.007

Kristensen, L.J., Taylor, M.P., Odigie, K.O., Hibdon, S.A., Flegal, A.R., 2014. Lead isotopic compositions of ash sourced from Australian bushfires. Environ. Pollut. 190: 159–165. https://doi.org/10.1016/j.envpol.2014.03.025

Landgate Fire Watch, accessed on 23.1.2021, https://firewatch-pro.landgate.wa.gov.au/

Lanteigne, S., Schindler, M., McDonald, A.M., Skeries, K., Abdu, Y., Mantha, N.N., Murayama, M., Hawthorne, F.C., Hochella Jr., M.F., 2012. Mineralogy and weathering of smelter-derived spherical particles in soils: implications for the mobility of Ni and Cu in the surficial environment. Water Air Soil Pollut. 223: 3619e3641. https://doi.org/10.1007/s11270-012-1135-3

Lentile, L.B., Holden, Z.A., Smith, A.M.S., Falkowski, M.J., Hudak, A.T., Morgan, P., Lewis, S.A., Gessler, P.E., Benson, N.C., 2006. Remote sensing techniques to assess active fire characteristics and post-fire effects. Int. J. Wildland Fire 15: 319-345. https://doi.org/10.1071/WF05097

Lodenius, M., Tulisalo, E., Soltanpour-Gargari, A., 2003. Exchange of mercury be- tween atmosphere and vegetation under contaminated conditions. Sci. Total Environ. 304: 169e174. https://doi.org/10.1016/S0048-9697(02)00566-1

Maier, W.D., Barnes, S.J., Chinyepi, G., Barton Jr., J.M., Eglinton, B., Setshedi, I., 2008. The composition of magmatic Ni-Cu-(PGE) sulfide deposit in the Taiti and Selebi-Phikwe belts of eastern Botswana. Miner. Depos. 4: 37-60. https://doi.org/10.1007/s00126-007-0143-5

Mihaljevič, M., Ettler, V., Vaňek, A., Penížek, A., Svoboda, M., Kříbek, B., Sracek, O., Mapani, B.S., Kamona, A.F., 2015. Trace elements and the lead isotopic record in marula (*Sclerocarya birrea*) tree rings and soils near the Tsumeb smelter, Namibia. Water Air Soil Pollut. 226: 177. https://doi.org/10.1007/s11270-015-2440-4

Mihaljevič, M., Ettler, V., Šebek, O., Sracek, O., Kříbek, B., Kyncl, T., Majer, V., Veselovský, F., 2011. Lead isotopic and metallic pollution record in tree rings from the Copperbelt mining-smelting area, Zambia. Water Air Soil Pollut. 216: 657–668. https://doi.org/10.1007/s11270-010-0560-4

Millhollen, A.G., Gustin, M.S., Obrist, D., 2006. Foliar mercury accumulation and exchange for three tree species. Environ. Sci. Technol. 40: 6001e6006. https://doi.org/10.1021/es0609194

Miranda, A.C., Miranda, H.S., Dias, I.F.O., Dias, B.F.S., 1993. Soil and air temperatures during prescribed cerrado fires in Central Brazil. J. Trop. Ecol. 9: 313-320. https://doi.org/10.1017/S0266467400007367

Muñoz-Rojas, M., Pereira, P., 2020. Editorial: Fire in the environment. J. Environ. Manage. 253: 109703. https://doi.org/10.1016/j.envman.2019.109703

NASA FIRMS, Fire Information for Resource Management System, accessed on 23.1.2021, https://firms.modaps.eosdis.nasa.gov/

Navrátil, T., Hojdová, M., Rohovec, J., Penížek, V., Vařilová, Z., 2009. Effect of fire on pools of mercury in forest soil, central Europe. Bull. Environ. Contam. Toxicol. 83: 269-274. https://doi.org/10.1007/s00128-009-9705-9

Neary, D.G., Klopatek, C.C., DeBano, L.F., Fjolliot, P.F., 1999. Fire effects on below ground sustainability: a review and synthesis. For. Ecol. Manage. 122: 51-71. https://doi.org/10.1016/S0378-1127(99)00032-8

Nriagu, J.O., 1989. A global assessment of natural sources of atmospheric trace metals. Nature 338: 47-49. https://doi.org/10.1038/338047a0

Odigie, K.O., Flegal, A.R., 2014. Trace metal inventories and lead isotopic composition chronicle a forest fire's remobilization of industrial contaminants deposited in the Angeles National Forest. PLOS One 9: e107835. https://doi.org/10.1371/journal.pone.0107835

Odigie, K.O., Flegal, A.R., 2011. Pyrogenic remobilization of historic industrial lead depositions. Environ. Sci. Technol. 45: 6290-6295. https://doi.org/10.1021/es200944w

Pausas, J.G., Keeley, J.E., 2019. Wildfires as an ecosystem service. Frontiers in Ecology and the Environment 17: 289-295. https://doi.org/10.1002/fee.2044.

Pereira, P., Mataix-Solera, J., Úbeda, X., Rein, G., Cerdà, A., 2019. Fire Effects on Soil Properties. CSIRO Publishing, Clayton South.

Pirrie, D., Rollinson, G.K., 2011. Unlocking the applications of automated mineral analysis. Geol. Today 27: 226e235. https://doi.org/10.1111/j.1365-2451.2011.00818.x

Rieuwerts, J.S., Farago, M., Cikrt, M., Bencko, V., 1999. Heavy metal concentrations in and around households near a secondary lead smelter. Environ. Monit. Assess. 58: 317-335. https://doi.org/10.1023/A:1006058331453

Ryan, K.C., 2002. Dynamic interactions between forest structure and fire behavior in boreal ecosystems. Silva. Fenn. 36: 13-39. https://doi.org/10.1139/X10-144

Ryan, K.C., Noste, N.V., 1985. Evaluating prescribed fires. In Proceedings, Symposium and Workshop on Wilderness Fire. 15-18 November 1983, Missoula, MT. (Eds Lotan J.E., Kilgore, B.M., Fisher, W.C., Mutch, R.W.) pp. 230-238. General Technical Report INT-182, USDA Forest Service, Intermountain Forest and Range Experimental Station, Missoula MT, USA.

Safarzadeh, M.S., Miller, J.D., 2016. The pyrometallurgy of enargite: a literature update. Int. J. Miner. Process. 157: 103–110. https://doi.org/10.1016/j.minpro.2016.09.008

Sankey, J.B., Kreitler, J., Hawbaker, T.D., McVay, J.L., Miller, M.E., Mueller, E.R., Vaillant, N.M., Lowe, S.E., Sakey, T.T., 2017. Climate, wildfire, and erosion ensemble foretells more sediment in western USA watersheds. Geophys. Res. Lett. 44: 8884-8892. https://doi.org/10.1002/2017GL073979

Scott, A.C., 2018. Burning Planet. Oxford University Press, ISBN 978-0-19-873484-0.

Scott, A.C., Chaloner, W.G., Belcher, C.M., Roos, C.I., 2016. The interaction of fire and mankind. Philos. Trans. R. Soc. B-Biol. Sci. 371: 20160149. https://doi.org/10:1098/rstb.2016.0149

Shakesby, R.A., Doerr, S.H., 2006. Wildfire as a hydrological and geomorphological agent. Earth-Sci. Rev. 74: 269-307. https://doi.org/10.1016/j.earscirev.2005.10.006

Sikamo, J., Mwanza, A., Mweemba, C., 2016. Copper mining in Zambia – history and future. J. S. Afr. Inst. Min. Metall. 116: 491-496. http://dx.doi.org/10.17159/2411-9717/2016/v116n6a1

Smith, A.M.S., Wooster, M.J., Drake, N.A., Dipotso, F.M., Falkowski, M.J., Hudak, A.T., 2005. Testing the potential of multi-spectral remote sensing for retrospectively estimating fire severity in African Savannahs. Remote Sens. Environ. 97: 92-115. https://doi.org/10.1016/j.rse.2005.04.014

Sracek, O., Kříbek, B., Mahaljevič, M., Ettler, V., Vaněk, A., Filip, J., Veselovský, F., Bagai, Z.B., 2018. Geochemistry and pH control of seepage from Ni-Cu rich mine tailings at Selebi Phikwe, Botswana. Environ. Monit. Assess. 190: 482. https://doi.org/10.1007/s10661-018-6851-8

Stavel, A.K., Archibald, S., Levin, S.A., 2011. The global extent and determinants of savanna and forest as alternative biome states. Science 334 (6053): 230-232. https://doi.org/10.1126/science.1210465

Stephens, S.L., Moghaddas, J.J., 2005. Experimental fuel treatment impacts on forest structure, potential fire behavior, and predicted tree mortality in a California mixed conifer forest. For. Ecol. Manage. 215: 21-36. https://doi.org/10.1016/j.foreco.2005.03.070

Sullivan, A.L., 2017. Inside the inferno: Fundamental Processes of Wildland Fire bahaviour. Curr. Forestry Rep. 3: 132-149. https://doi.org/10.1007/s40725-017-0057-0

Tembo, B.D., Sichilongo, K., Cernak, J., 2006. Distribution of copper, lead, cadmium and zinc concentrations in soils around Kabwe town in Zambia. Chemosphere 63: 497–501. https://doi.org/10.1016/j.chemosphere.2005.08.002

Tyszka, R., Pietranik, A., Kierczak, J., Ettler, V., Mihaljevič, M., Medynska-Juraszek, A., 2016. Lead isotopes and heavy minerals analyzed as tools to understand the distribution of lead and other potentially toxic elements in soils contaminated by Cu smelting (Legnica, Poland). Environ. Sci. Pollut. Res. 23: 24350e24363. https://doi.org/10.1007/s11356-016-7655-4

Úbeda, X., Pereira, P., Badía, D., 2018. Prescribed fires. Sci. Total Environ. 637-638: 385-388. https://doi.org/10.1016/j.scitotenv.2018.04.272

Úbeda, X., Pereira, P., Outeiro, L., Martin, D., 2009. Effects of fire temperature on the physical and chemical characteristics af the ash from two plots of cork oak (Quercus suber). Land Degrad. Dev. 20: 589-608. https://doi.org/10.1002/ldr.930

USGS, 2020. Mineral commodity summaries 2020: U.S. Geological Survey, 200 p., https://doi.org/10.3133/mcs2020

USGS, Controlled fire studies provide data on archaeological sites impacts, accessed on 11.5.2021, https://www.usgs.gov/media/images/controlled-fire-studies-provide-data-archaeological-sites-impacts

Uzu, G., Sobanska, S., Aliouane, Y., Pradere, P., Dumat, C., 2009. Study of lead phytoavailability for atmospheric industrial micronic and sub-micronic particles in relation with lead speciation. Environ. Pollut. 154: 1178e1185. https://doi.org/10.1016/j.envpol.2008.09.053

Webster, J.P., Kane, T.J., Obrist, D., Ryan, J.N., Aiken, G.R., 2016. Estimating mercury emissions resulting from wildfire in forests of the Western United States. Sci. Total Environ. 568: 578e586. https://doi.org/10.1016/j.scitotenv.2016.01.166

Weinhold, B., 2011. Fields and forests in flames: vegetation smoke and human health. Environ. Health Perspect. 119: A236-A393. https://doi.org/10.1289/ehp.119-a386

Westerling, A.L.R., 2016. Increasing western US forest wildfire activity: sensitivity to changes in the timing of spring. Philos. Trans. R. Soc. B-Biol. Sci. 371: 20150178. https://doi.org/10.1098/rstb.2015.0178

Wiedinmeyer, C., Friedli, H., 2007. Mercury emission estimates from fires: an initial inventory for the United States. Environ. Sci. Technol. 41: 8092-8098. https://doi.org/10.1021/es071289o

Wilson, I.H., 2018. Provenance of lead (Pb) in soils in the Mt Isa urban area. Appl. Geochem. 93: 113-128. https://doi.org/10.1016/j.apgeochem.2018.04.007

Wisconsin Department of Natural Resources, Prescribed burns spart a better future for rare ecosystems, accessed on 11.5.2021, https://dnr.wisconsin.gov/newsroom/release/40611

Wu, Q., Wang, S., Wang, L., Liu, F., Lin, C.J., Zhang, L., Wang, F., 2014. Spatial distribution and accumulation of Hg in soil surrounding a Zn/Pb smelter. Sci. Total Environ. 496: 668e677. https://doi.org/10.1016/j.scitotenv.2014.02.067

Yin, X., Yao, C., Song, J., Li, Z., Zhang, C., Qian, W., Bi, D., Li, C., Teng, Y., Wu, L., Wan, H., Luo, Y., 2009. Mercury contamination in vicinity of secondary copper smelters in Fuyang, Zhejiang Province, China: levels and contamination in topsoils. Environ. Pollut. 157: 1787e1793. https://doi.org/10.1016/j.envpol.2009.02.018